A Simplified Approach to Condensed Phase Combustion Modeling

Frederick Paquet

A thesis

in

The Department

of

Mechanical and Industrial Engineering

Presented in Partial Fulfillment of the Requirements

for the Degree of Master of Applied Science (Mechanical Engineering) at

Concordia University

Montréal, Québec, Canada

April 2008

Canada

Abstract

A Simplified Approach to Condensed Phase Modelling

Frederick Paquet

The combustion modeling of energetic materials still involves a guessing step due to the lack of knowledge in the condensed phase. Quantum dynamical calculations are presently the only way to predict the initial gasification reaction but require tremendous computing power, thus limiting their application. This constitutes a lack of completeness in the design of modeling tools. Through quantum mechanics, it is known that incoming energy will couple only in certain ways with a molecular system. The way this coupling is defined will depend on the selection of an energy model. A simple empirical method was devised which uses an energy coupling assumption and spectroscopic data of energetic molecules as the source for the complete modal molecular picture of the system. The method enables a qualitative prediction of the first combustion reaction through comparison with emission spectra of energy sources. The goal of this work is to present the method developed along with some results and gather tools for future research in the same subject. The thesis will first review the current state of research in the field of condensed phase energetic materials combustion. A discussion on the different theoretical foundations and assumptions used related to quantum mechanics and spectroscopy shall follow culminating with a description of the method developed. The analysis method will then be applied with two example energetic molecules nitroguanidine and nitrocellulose. The study will conclude with an explicit prediction for the two example cases followed by a discussion on future research that could be undertaken based on the conclusions drawn here.

Résumé

Une Approche Simplifiée pour la Modélisation de la Phase Condensée

Frederick Paquet

La modélisation de la combustion des matériaux énergétiques requière encore une étape de supposition en raison du manque de connaissance sur la phase condensée. Les calculs appliqués de dynamique quantique sont présentement la seule manière de prédire la réaction initiale de conversion en gaz mais ces derniers requièrent une puissance informatique très importante. Cette situation démontre un manque dans la conception des outils de modélisation. La mécanique quantique nous montre que certains niveaux d'énergie très précis sont absorbés par un système moléculaire. La valeur de ces niveaux dépend du type de modèle d'énergie potentielle choisis. Une méthode empirique simple fut développée à l'aide d'une hypothèse de couplage de l'énergie et de données spectroscopiques de molécules énergétiques. La spectroscopie est prise ici comme l'image modale complète d'un système moléculaire. La méthode permet une prédiction qualitative de la première réaction lors d'une combustion par une comparaison avec les spectres d'émission de différentes sources d'énergie. Le but de ce travail est de présenter la méthode avec quelques résultats ainsi que d'acquérir les outils qui nécessaires à la continuation de cette recherche. Cette thèse révisera premièrement l'état présent de la recherche dans le champ de la combustion en phase condensée. Une discussion sur les différentes fondations théoriques relevant de la mécanique quantique et de la spectroscopie suivra et culminera avec une description de la méthode proposée. La méthode d'analyse sera par la suite appliquée avec deux molécules énergétiques : la nitroguanidine et la nitrocellulose. Cette étude sera finalement conclue par une prédiction de la première réaction des cas utilisés en exemple et discutera des contributions futures possibles à cette recherche.

Acknowledgments

Contents

Contents

Contents

List of Figures

List of Figures

List of Tables

Glossary

A_s	Pre-exponential constant
c	Speed of light
E	Energy
E_d	Dissociation energy
E_s	Activation energy
h	Planck's constant
h_i	Species enthalpy
k	Spring constant; Wave number
k_b	Boltzmann's constant
I	Moment of inertia
J	Rotational quantum number
$\dot{m}$	Gasification rate
n	Quantum number
n_v	Vibrational quantum number
R	Ideal gas constant
x	Single dimension of the system
t	Time
T	Temperature
V	Potential energy
Y_i	Species mass fraction
Z	Partition function

Acronyms

DEGDN	Diethylene glycol dinitrate
DSC	Differential scanning calorimeter
FTIR	Fourier transform infraRed
GN	Guanidine nitrate
HMX	Cyclo-tetramethylene-tetranitramine
MURI	Multidisciplinary university research initiative
NC	Nitrocellulose
NG	Nitroglycerine
NQ	Nitroguanidine
PREMIX	Chemkin premixed flame code
RDX	Cyclo-trimethylene-trinitramine
TAGN	Triaminoguanidine nitrate
TEGDN	Triethylene glycol dinitrate
TMETN	Trimethyloletane trinitrate
TGA	Thermo-gravimetric analysis
SEM	Scanning electron microscopy

Greeks

ν	Frequency
ν_o	Fundamental frequency
λ_g	Thermal conductivity
λ	Wave length

Chapter 1

Introduction

1.1   General overview

The modern requirements for applications such as rockets, airbags inflators and guns are changing how new propellants are formulated. Traditional ingredients, such as nitrocellulose (NC) and nitroglycerine (NG) are no longer able to always provide valid solutions to meet specifications. In order to modernize propellant formulation, a great deal of research is being done to discover and test new energetic molecules. In addition, theoretical and empirical knowledge is being increasingly coupled with the power of computers to predict the burning behaviour of propellants. In that aspect, the application of gaseous phase chemistry has been quite successful in representing the reality. However, the gas phase processes correspond often only the second part of the combustion phenomenon. The beginning of combustion occurs in the condensed phase of the material in most cases. The reactions occurring in the condensed phase dictate what could possibly happen in the gas phase. Nowadays, due to a lack of theoretical and experimental knowledge, the condensed phase reactions are usually derived from educated guesses (Beckstead, 2006). It has been shown that different condensed phase reactions can yield very different burning behaviour because of a number of possible reaction paths (Miller and Anderson, 2000). A theoretical understanding of condensed phase processes in the combustion of propellants could therefore enable one to design a propellant system

1

that would use a wanted reaction path in order to get a precise defined burning behaviour. The development of a general method to predict the initial condensed phase decomposition reaction is the general goal of this research.

1.2 Basics of propellant combustion

One of the most important propellant parameter is its burning rate (usually measured in units of distance per unit time). Altough the energy content of a given formulation is also an important parameter, a high energy content does not imply a high burning rate. A good example of this is the case of RDX (cyclo-trimethylene-trinitramine). While RDX has interesting thermodynamic properties and a high energy content, its burning rate is fairly low and thus limits greatly the number of applications in which it can be used with success. The capability to accurately predict burning rates (or gasification rates) for different propellants has been one of the main thrusts in the energetic material combustion research effort. It is currently required to manufacture enough of a given propellant to be able to test it in a closed vessel and measure the burning rate. This is a costly and time consuming process. Furthermore, using empirical correlations built by the experience of repeating the above process does not at all bring a level of understanding comparable to theoretical knowledge.

In the last two decades, combustion modelling of propellants has been done using mostly similar basic steps. The process is divided into three phases: solid, condensed and gaseous (Beckstead, 2006). This is illustrated in figure 1.1. The conservation relations (mass and energy) are solved for all three zones and a set of boundary conditions are applied between the zones. Usually, only the energy equation is solved in the solid phase to model the convection and conduction heat transfer as no chemical reactions are assumed there (Beckstead, 2006).

In the thin condensed phase zone, the reactants are taken as liquids and gas bubbles are present due to the gasification process taking place there (Schroeder et al., 2001). Hence molecular diffusion is an important component and is included in the mass conservation relation. Several modelling philosophies have been used to simulate the processes taking place in
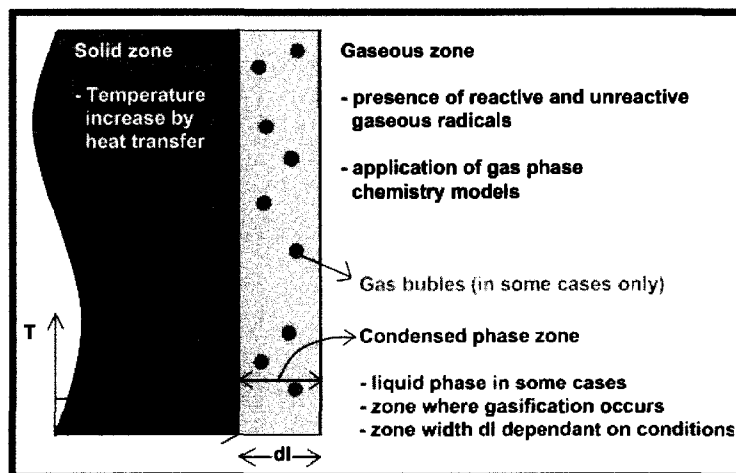
Figure 1.1. Schematic of the physical phases found in a combustion

the condensed phase. In most cases, the mechanical structure inside the liquid with dissolved gaseous products is modelled to solve the conservation relations (Liau et al., 1995). In all cases, the chemical reactions taking place there are not well known and must usually be determined intuitively or by limited experimental knowledge. A pyrolysis law, shown in equation 1.1, in the form of an Arrhenius relation, is used to model the kinetics of the reactions with respect to the temperature (Zenin, 1995):

$$\dot{m} = A_s e^{-E_s/RT} \tag{1.1}$$

where $\dot{m}$ is the gasification rate, R the ideal gas constant, and T the temperature of the condensed phase surface. The activation energy and the pre-exponential coefficient (E_s and A_s respectively) are obtained by measurements.

Miller and Anderson have collapsed the condensed phase to a boundary condition by neglecting both diffusion and the liquid phase in addition to assuming that chemical reactions occur at the solid-gas interface (Miller and Anderson, 2000). These simplifications enabled them to reduce the energy conservation equation to the following simple form in the condensed

phase:

$$\lambda_g \left(\frac{dT}{dx} \right) = \dot{m} \sum_i^N \left(Y_i^{-0} h_i^{+0} - Y_i^{-\infty} h_i^{-\infty} \right) \tag{1.2}$$

where λ_g is the thermal conductivity of the gas phase, T is the temperature, $\dot{m}$ is the gasification rate (mass of gas produced per unit time), Y_i is the mass fraction of the ith species, h_i is the enthalpy of the ith species and x is the single dimension of the system. Note that the superscripts "$-\infty$" and "-0" and "$+0$" relate to the unreacted propellant, the condensed phase side of the surface and the gas phase side of the surface respectively. This modelling method by Miller and Anderson has the virtue of greatly simplifying the condensed phase analysis while yielding accurate results. The two authors have published results of linear burning rate predictions using their model for single, double and triple base propellants (Miller and Anderson, 2004) containing a variety of widely used energetic materials such as nitrocellulose, nitroglycerine, nitroguanidine, RDX (Cyclo-trimethylene-trinitramine), and DEGDN (diethylene glycol dinitrate). Their results were shown to be in agreement with experimental data but were dependent upon the chosen initial condensed phase reaction (Miller and Anderson, 2000). Hence the method remains an empirically-based one.

The conservation relations are usually solved using a combustion simulation code such as PREMIX (Kee et al., 1985). In fact, Miller and Anderson used a modified version of PREMIX as a subroutine in their modelling system (Miller and Anderson, 2000). For propellant simulations there is a much better understanding of gas phase phenomena during combustion; this is why the methods used there are more standard.

It appears that modelling the combustion of propellants is not an easy matter due to the lack of theoretical and experimental understanding of condensed phase processes. There are many research groups that currently devote their studies to the molecular dynamics of condensed phase energetic materials combustion. The MURI (Multidisciplinary University Research Initiative) Accurate Theoretical Predictions of the Properties of Energetic Materials research group is a good example. The subject however remains very challenging and major advancements have been limited. Hence, important work should be done to better understand condensed phase processes during combustion in order to improve the modeling and control

the phenomena.

1.3   Condensed phase combustion

1.3.1   Theory and modelling

Condensed phase reactions have become an important subject of recent combustion research (Sorescu et al., 2003). It is a multidisciplinary subject that involves heat transfer, fluid mechanics, statistical thermodynamics, and quantum chemistry. The greatest challenge encountered yet has been to accurately model the molecular reactions. This difficulty arises from the complexity of solving the equations of quantum mechanics for the large systems under study. As can be observed in any quantum mechanics litterature, calculating the electronic parameters of the hydrogen atom is already very complicated (Pilar, 2001). Hence, the fact that most energetic molecules most often comprised of 10 atoms or more renders the computations extremely difficult.

Molecules are systems composed of atomic nuclei and electrons. The behaviour of such systems is described by a conservation relation known as the Schrödinger's equation. It is however quite helpful for computational purpose to decouple the nuclear and electronic parts of the equation. This is known as the Born-Oppenheimer approximation and is warranted by the smallness of the election mass compared to that of the atomic nucleus. Hence the system is usually solved by assuming stationary nuclei and allowing electrons to freely move in the potential field (Pilar, 2001). This enables one to predict how chemical bounds will form, the energy they contain and what shape the molecule will have. One must however realize that even if such approximations are used, the complexity of solving Schrödinger's equation has made it impossible until recently to study the molecular dynamics of more complex molecules such as those found in energetic materials (Sorescu et al., 2003).

In order to more easily study chemical reactions, scientists have devised the concept of potential surfaces. Such surfaces are simply 3-dimensional plots of the potential energy against the atomic distances between 3 components of the molecular system (Levine, 2005). Since chemical reactions involve bonds breaking and atomic distances changes, it follows that any line on a potential surface will represent a certain reaction. Such a line is called a reaction path

in molecular dynamics (Levine, 2005). If no external forces are present, a reaction will strive to attain the minimum equilibrium energy possible. One can thus study potential surfaces of a given energetic material to determine which bound is likely to break first. The limits of computing power restrict the possible dimensionality of the problem (number of molecular components that can be studied at the same time). Furthermore, since potential surfaces are calculated from empirical observations (for an approximation purpose), errors will come from the particular empirical models chosen (Sorescu et al., 2003).

The methods discussed above are equally valid in the treatment of gas phase or condensed phase phenomena. In the condensed phase (liquid and/or solid), the structure of the substance (e.g.: long liquid polymer chains, crystals, etc.) must also be considered as it will influence its physical properties and how it will absorb energy.

Solids consist of molecules arranged together in a more or less orderly fashion with cohesion due to the electrostatic force between molecules (not by chemical bounds) (Dlott, 2003). Given the nature of solids, there are two possible excitation modes possible: translation and vibration. It is important to differentiate between the processes linked to each of these modes. It has been reported that shock waves (such as those found in detonations) will affect the translational modes of the molecules within the solid (Dlott, 2003). This shows the phenomena to be more of a mechanical energy transfer. In the case of deflagration processes, the vibrational modes will be exited due to the thermal energy transferred to the unburned material. Hence it apparently becomes useful to separate shock and thermal energy transfer causes in the theoretical studies (Dlott, 2003). In the case of propellants, there is strictly thermal energy transfer (although shock waves are quite possible but extremely unwanted in this case).

Extensive studies are currently being made to better understand the geometric structure of solid energetic materials. Knowing the microscopic geometrical shape of these crystals enables one to calculate the different excitation modes of the material. Early models considered only rigid molecules and thus neglected intra-molecular vibrations. However, such models are not useful as they do not describe well the conditions encountered in the high pressures and

temperatures characteristic of combustion (Sorescu et al., 2003). In order to better capture the vibrational behaviour, potential energy surfaces (such as the well known Morse potential) are used. By combining the knowledge of both inter and intra molecular modes, a more complete picture of the material under study is obtained. One can then solve the Schrodinger's equation in a molecular dynamics simulation and determine how the energy input will affect the system (Dlott, 2003). Again, it must be stressed that such calculations have only recently become possible to perform with an acceptable precision due to the computing power required.

In the case of liquids, things become more complicated as rotation must be taken into account. The description of liquids is more difficult as they exhibit properties common to both gases and solids. It is therefore hard to use approximations that would neglect any of these important properties (Hill, 1987) and the analysis that is already tedious for the simpler cases becomes almost impossible for the moment. There would however be a lot to be gained from a better understanding of liquid state combustion as many energetic materials are used in a liquid form (such as NG and DEGDN) and a large number of the others are suspected to decompose after the fusion to their liquid state (Schroeder et al., 2001).

From the above discussion, it becomes clear that the current state of the art condensed phase theory and modelling is extremely complex. The molecular structures and reactions are derived directly from pure quantum mechanics by making a few relevant assumptions to simplify the computations (Sorescu et al., 2003). There is no mention of any simpler theory or method that would be valid for condensed phase combustion. In other words, this resembles the case where one would be using the general theory of relativity to launch a spacecraft in orbit rather then classical mechanics. It would be desirable to search for simpler methods based on what is already known (which would offer many engineering perspectives). One can note here the advantage that the more complete and general theory is already known (compared to the case of classical and relativistic mechanics).

1.3.2 Experimental investigations

Although the empirical study of condensed phase combustion processes have always been deemed as difficult, there have been several interesting studies on the subject. The most successful methods have been mostly revolving around thermal analysis, spectroscopy and microscopy. A coupling of these methods with the knowledge of the thermodynamics of the reactant and possible products enabled researchers to emit some significant hypothesis about condensed phase reactions.

The physico-chemical study of propellants with a quenched reaction surface using scanning electron microscopy (SEM) and Fourier transform infrared (FTIR) microscopy has been attempted, as shown by a recent string of publications by Schroeder et al. (2001). The visual SEM analysis enabled the authors to distinguish the different phases that were present at the time of quenching (liquid, amorphous solid, crystalline solid) in cross sections of the material. FTIR microscopy produced a spectrum of these sections that could be compared to the spectrum of unburned material samples and to chemical bounds spectral references. For example, the appearance of certain bands or the decrease in the amplitude of others in the spectrum is directly related to the presence of certain chemical groups and bounds. The knowledge of the groups present at the quenching can be used to determine what intermediate reactions could have taken place with more precision (Schroeder et al., 2001).

A very interesting and simple approach concerning the decomposition of triaminoguanidine nitrate (TAGN) was suggested by Kubota et al. (1988). Their method involved thermogravimetric (TGA) and differential scanning calorimeter (DSC) measurements. The DSC measurements showed the phase change from solid to liquid followed by a multi-stage exothermic decomposition. The TGA measured the mass losses from solid-liquid to gases. Combining the two measurements gave a serious hint that the main energetic property of TAGN arises from the initial breakage of the three NH_2 bounds. This conclusion comes from the match in the mass fraction of the amino groups and the mass loss measured by TGA (Kubota et al., 1988). Comparison with the same measurements done on the brother-substance of TAGN, guanidine nitrate (GN), and thermodynamical data enabled to reinforce the conclusions of the

researchers. Continuing the reaction of a TAGN sample that had its combustion quenched after the initial amino loss showed the expected resemblance with GN when looking at the DSC and TGA profiles (Kubota et al., 1988).

It can be seen here that the discussed techniques do not show directly the condensed phase chemical processes occurring but enable one to deduce what happens. Indeed, there has not been much success in trying to study the direct products of condensed phase processes due to the temporary nature of these products and especially the difficult pressure/temperatures at which they must be measured. Complex apparatus, such as that featured in a study by Korobeinichev (2000), would present an extremely interesting alternative if it could work in harsher conditions. The more simple approaches discussed here would however be useful in verifying future theoretical predictions.

1.4   Current knowledge about energetic molecules

Following the previous general discussions, it is interesting to look at some energetic substances and what has been discovered about their condensed phase combustion in more details using the techniques and theorie that have been presented. The conclusions and ideas presented in this section will serve as a mean of validation to the calculations that shall be made later in this study with certain energetic molecules. It must be noted again that the initial condensed phase reactions of different energetic molecules described here are not at all completely proven as true but are currently regarded as the most probable ones.

Energetic compounds are divided into families based on the structure of their molecules and the presence of some chemical groups and bonds. All members of these families have some similar characteristics during their combustion due to the molecular groups common to them. Two categories that are widely used in propellant formulations, nitramines and nitrate esters, are further discussed here.

1.4.1 Nitramines

The main feature of nitramines is their hydrocarbon-like structure containing several $N-NO_2$ chemical bounds (Kubota, 2007). At standard temperature and pressure, they are in a crystalline form. Their combustion involves a change of phase to liquid and, to some extent, gaseous form.

Among the nitramines, cyclo-trimethylene-trinitramine RDX is a widely used substance in many explosives, propellants and gas generating compositions. Its condensed phase combustion is still quite misunderstood even if it has been quite extensively studied. What is known with certainty is that a burning RDX sample consists of a cool solid propellant zone, a heating zone still in the solid phase and a liquid phase containing gas bubbles. The length of this liquid layer decreases with increasing pressures (Schroeder et al., 2001). The composition of the gas bubbles is not certain and is the main source of the problem. Most researchers now believe that the bubbles are made of RDX vapour (Miller and Anderson, 2000). Others claim that they consist more of a mixture of decomposition products and RDX vapour (Schroeder et al., 2001). This is important as the initial reaction involved to decompose a liquid or a gas will be different. The main argument used to defend the liquid phase decomposition is that RDX melts at 204°C, starts decomposing at 227°C and is estimated to boil at 391 +/- 33°C (Schroeder et al, 2001). The vapour phase decomposition hypothesis was applied in the burning rate prediction model of Miller & Anderson (Miller and Anderson, 2000) with a fairly good success. The actual chemical decomposition reaction is not known in the liquid phase for the moment as this process in not favoured by researchers.

Another nitramine is Cyclo-tetramethylene-tetranitramine (HMX). The combustion of HMX seems to be much more understood then that of RDX as judged by the number of publications and their clarity. Kubota reports (Kubota, 2007) that the initial decomposition reaction of HMX is the following:

$$3(CH_2NNO_2)_4 \rightarrow 4NO_2 + 4N_2O + 6N_2 + 12CH_2O \qquad \text{(R-1)}$$
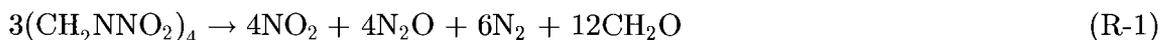
Differential scanning calorimeter and thermo-gravimetric analysis measurements have shown

that this reaction is likely to occur in the liquid phase (Kubota et al., 1989). Furthermore, FTIR analysis has helped to confirm that the decomposition reaction begins with the breaking of the N-NO$_2$ bond, thus yielding reaction R-1 (Kubota et al., 1989). The condensed phase again contains gas bubbles with the initial reaction products along with possible further gas-phase reactions products. Like RDX, the liquid phase layer is shown to decrease in length with increasing pressure (Schroeder et al., 2001).

The last nitramine discussed is nitroguanidine (NQ), which is a common triple base propellant ingredient. NQ is a crystalline solid usually used as energetic filler in triple base propellants because of the low molecular weight of its combustion gases and its low flame temperature. Most research on this substance tends to favour the breaking of all single bonds as an initial reaction (Volk, 1985). In their modelling effort, Miller & Anderson have found that the reaction yielding the best burning rate results is the following (Miller and Anderson, 2004):

$$NQ(solid) \rightarrow NO_2 + HCN + NH_2 + NH \qquad \text{(R-2)}$$

Observation of R-2 confirms the breaking of single bonds. The reaction is assumed to be occurring in the solid phase as NQ has a melting point of 255°C and a decomposition temperature of 250°C (Miller and Anderson, 2004). As seen in R-2, the presence of hydrogen rather then oxygen in the initial gaseous products is the reason for the low molecular weight of these gases.

1.4.2 Nitrate esters

The family of nitrate esters represents another type of energetic compounds. This group contains the most widely used compounds in propellant ingredients (nitrocellulose and nitroglycerin are the main ones). The currently most important nitrate esters are nitroglycerin, nitrocellulose, diethylene glycol dinitrate, triethylene glycol dinitrate, and trimethyloletane trinitrate (NG, NC, DEGDN, TEGDN, and TMETN respectively). They have in common the energetic O-NO$_2$ bonds in their hydrocarbon structure. It is this bond that is suspected

to break first during combustion (or decomposition) (Kubota, 2007). Various nitrate esters molecules contain different amounts of $O\text{-}NO_2$ bonds, which explain their various energy contents (Kubota, 2007). NC itself can have a varying percentage of $O\text{-}NO_2$ bonds (typically between 11 and 14% is used) depending on the nitration process done on cellulose. This is of importance as different applications will require different types of NC. Furthermore, this incomplete nitration coupled with the polymer structure of NC molecules renders theoretical modelling of its combustion challenging (Miller and Anderson, 2004).

Although the initial reaction common to nitrate esters discussed above is widely accepted, the global molecular dynamics of this reaction evolution is still quite unknown as of yet. A most striking example of this situation was described by Miller and Anderson in their modelling of NG (Miller and Anderson, 2000). In that example, the three following condensed phase NG decomposition reactions were analyzed from various sources (Miller and Anderson, 2000):

$$NG(C_3H_5N_3O_9) \rightarrow 3NO_2 + 2CH_2O + HCO \tag{R-3}$$

$$NG \rightarrow 2NO_2 + HONO + 2CH_2O + CO \tag{R-4}$$

$$NG \rightarrow 3HONO + 2HCO + CO \tag{R-5}$$

Through modelling of the burning rate, it was found (Miller and Anderson, 2000) that R-5 yielded results in agreement with empirical data (with variations of an order of magnitude when choosing other reactions). It can be observed in the previous three reactions that the main difference is the bonds breaking sequence. R-3 has all $O\text{-}NO_2$ and C-C bounds breaking, thus initially transforming NG into gaseous products. The other two reactions have differing degrees of interaction between gaseous and condensed phase products. This shows quite clearly how a better understanding of condensed phase combustion molecular dynamics could help the modelling and possibly control of the phenomena (Miller and Anderson, 2000). It must be noted that, like nitramines, nitrate esters also exhibit a liquid reaction zone containing gas bubbles (Schroeder et al., 2001). It is however not yet determined if the bubbles contain gasification products or simply evaporated nitrate esters.

1.4.3 General observations on energetic compounds categories

Through the description of the previous families, some similarities can be observed in the initial reactions proposed. Nitramines are expected to have their N-NO$_2$ bonds breaking first. In the case of nitrate esters, the O-NO$_2$ bonds are theorized to be the first ones to break. It can be noted that the defining groups of these families are the same than those currently predicted to break first in the combustion reaction. It is noteworthy to mention that other families will have their own particularities. Azides, for example, are theorized to have their distinctive N=N bonds ruptured first (Kubota et al., 1988). The specific behaviours intrinsic to each category are the reason why it is helpful to look at energetic molecules within the framework of these categories. Using these families can help one to select substances with expected differences in their combustion behaviour to study.

1.5 Objective of the present study

The initial bond breaking reactions discussed previously are widely accepted but there are no accurate theoretical predictions or direct experimental evidence available currently to support these claims. Furthermore, as was shown in previous sections, the dynamics of the molecular process is even less known. Hence, one of the most fundamental problems in condensed phase combustion is the nature and order of the initial reactions that take place. Given that the occurrence of a chemical reaction is controlled by the energy input to a given molecule, the question of how this energy couples with molecules becomes primordial. By energy coupling with the molecule, it is meant that the input energy will excite some specific modes depending on the nature of the energy and the modes. The now usual path taken to solve this is through molecular dynamics. This path suffers from its complexity and that last characteristic is currently the main reason why there are gaps in our knowledge of combustion phenomena. Therefore, this limits the modelling effort so crucial to design efficient engineering applications.

The first step in understanding and developing a simpler theory to solve problems in condensed phase combustion is to gather several fundamental tools that shall serve as the

foundation of any method obtained through this path. In addition to presenting the different theoretical and empirical tools gathered, this thesis will address the following question as a first application: *how does the input energy couple with a material to excite different modes and eventually break chemical bonds?* Using the solution to that problem in formulating simple predictions of how combustion reactions will initially proceed can be used as an informal verification of the method developed.

The tools required to address the main question shall be obtained by a thorough review of molecular modes and basic quantum mechanics concepts. Spectroscopic data shall be used as the modal signature of energetic molecules instead of the complex quantum mechanical calculations. Through this, it will become possible to have another view of condensed phase combustion and study the ignition process of energetic molecules.

Chapter 2

Molecular Modes and Spectroscopy

In this research, a method is proposed that uses fundamental quantum mechanics concepts and the understanding of molecular modes as a way to predict the coupling of input energy with energetic substances. Spectroscopy is used to get the information about the different mode of molecular systems. Furthermore, the knowledge of fundamental modes gained through spectroscopy will become very important in a later stage of the research which will look into the statistics of these dissociation reactions in order to obtain more information about the condensed phase processes. Therefore, the technique is virtually a diagnostic tool to quickly assess the modal excitation of a condensed phase energetic material system given an input of energy and determine if the occurrence of dissociation is possible. In order to obtain such a method, a number of simplifying assumptions are necessary. This chapter will discuss and validate the different assumptions required, review the theory of molecular modes and make the link with spectroscopy. From these discussions, the general method to follow will appear and shall be given explicitly.

2.1 Fundamental concepts and method approach

Given what is already known about molecular structure from quantum mechanics and empirical data, there are grounds to believe that there might be a way to elucidate the energy coupling issue by a mean simpler than the traditional molecular dynamics methods. The following three fundamental concepts will be used as an important starting point for the concept of a method:

- It is central to quantum theory, or any wave-based theory that wavelengths will couple if the smaller ones are integral fractions of the largest (i.e. the classical concept of resonance) (Pilar, 2001).

- Chemical bonds will break if sufficient excitation of their vibrational and/or electronic modes is achieved (Pilar, 2001).

- The set of excitation mode frequencies is known for a given substance through molecular spectroscopy (Laidler et al., 1982).

The above statements lead to the present proposed method, which uses spectroscopic data to determine the base vibrational frequencies of bonds. The coupling scheme is then applied to calculate the possible excitation wavelengths (or overtones). Hence, computational molecular dynamics is replaced by spectroscopic analysis in order to get the complete modal signature of a molecule. This in itself is an important simplification that will be warranted by the final results obtained.

2.2 Assumptions used in the method

Several assumptions must be made in order to simplify the analysis that will follow. Such hypotheses are necessary to link spectroscopic modal measurements with energy and to determine the point of bond scission. These assumptions are:

1. The input energy is quantized following Planck's law,

$$E = nh\nu \tag{2.1}$$

   where n is a positive integer called the quantum number, ν is the frequency and E is the energy (Pilar, 2001). Note that an amount of energy of size given by the above law is denoted as a photon.

2. The molecular bonds only dissociate through the excitation of vibrational modes.

3. The fundamental vibrational modes of a bond are determined by the inspection of infrared spectroscopy data.

4. A mode will only be excited by a photon if half of its wavelength is an integral multiple of the input photon wavelength.

5. A given bond is broken when the input photon has a wavelength matching or lower then that which corresponds to the dissociation energy of the bond.

Some important points must be brought forward concerning these assumptions. The first statement is the important link between energy and frequency (or wavelength) that has been discovered in 1900 by Planck and proven valid on many occasion since then. The second hypothesis greatly simplifies the process as it enables neglecting electronic modes and lattices modes in the solid case. It must be noted that a more complete analysis should include these modes. It was however thought to be beneficial to perform this simplified analysis as a first level application of the method. Electronic modes spectroscopy shall however be discussed later as it will be necessary to know the boundary of the vibrational excitation zone. The fourth assumption is the energy coupling assumption and shall be discussed in more details in the next section. The last hypothesis is simply the application of Planck's law to determine the frequency that will correspond to the dissociation energy of the bond.

2.3   The energy coupling assumption

In this case, the term energy coupling refers to how energy will be absorbed by the molecular system. That concept is usually denoted as the potential energy model in the chemical and physical literature. It was however judged useful to use the term energy coupling here as it illustrates more the goal of this research. In order to use it further, the energy coupling assumption requires some sort of proof of validity. To obtain that proof, it is useful to look at the specific model related to the system under study. Following the second assumption discussed previously, only the vibrational case is considered here.

When modelling molecular systems, the Born-Oppenheimer approximation is widely used to decouple the motion of the electrons and nucleus in the solution of the Schrodinger equation (Pilar, 2001). In the part of the solution that considers the atomic nucleus motion, the vibrational modes are modelled using the classical harmonic oscillator as a basis (two masses, atoms in this case, linked together by a spring that follows Hook's law). This system has potential energy

$$V(x_1, x_2) = k(x_1 - x_2)^2/2 \tag{2.2}$$

where x_1 and x_2 are the position of the atoms and k is the spring constant, which is related to the angular momentum in this case and which ultimately plays an important role in determining the fundamental frequency, ν_o, of the system. This potential is simply applied in the Schrodinger equation and the solutions are as follows:

$$E_v = (n_v + \frac{1}{2})h\nu_o \tag{2.3}$$

where the vibrational quantum number can take the values $n_v = 0$, 1, 2, etc. Here, it is seen that the solution is a first order approximation quantized through the parameter n_v and this comes from the solution of the Schrodinger partial differential equation (Pilar, 2001).

The quantum harmonic oscillator is, however, not the most precise model for molecular bonds. Spectroscopic observations show that the vibrational modes overtones are slightly anharmonic (Laidler et al., 1982). This means that the energy levels are not equally spaced
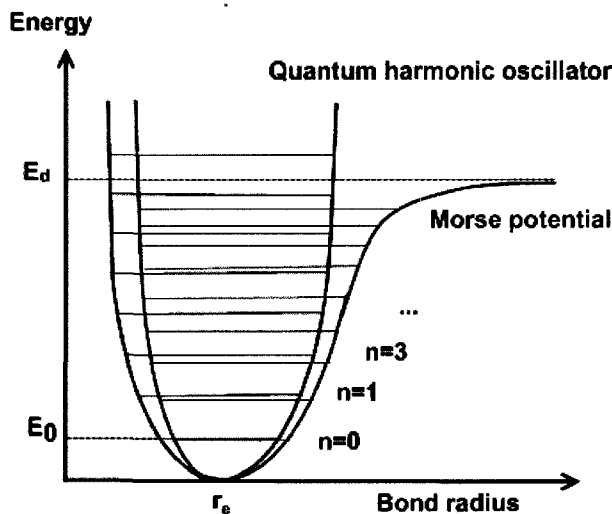
Figure 2.1. Comparison of the quantum harmonic and Morse potential curves

such as would be required by the energy coupling assumption. The observations show that the difference between consecutive levels decreases as energy increases. Phillip M. Morse modelled this behaviour using a second order approximation potential function. The result is the famous Morse potential curve shown on figure 2.1. This function has the advantage of predicting a dissociation energy represented as an horizontal asymptote on the curve. The anharmonicity property thus enables more energy levels than predicted by the harmonic oscillator to exist close to the dissociation limit. The region above the dissociation energy is not described by the Morse potential function as it is considered outside of the potential well. In this region, the particles are taken as free and the solution of the Schrodinger equation does not yield quantized energy levels (i.e. there is a continuum of energy) (Laidler et al., 1982).

It is important here to remember that the method being discussed in this case is an empirical one that will use literature values of dissociation energies. Furthermore, the prime goal of using one of the quantized vibrational oscillator model is to determine frequencies that will be closest to the dissociation limit starting from spectroscopic data. Hence, having precise intermediate values is not important for this case. Such would not be the case if, for example,

it would be necessary to calculate the partition function of the vibrational energies in order to use it to compute thermodynamical properties.

The vibrational energy quantization scheme described above is directly compatible with the energy coupling hypothesis and thus confirms its validity in this case. In addition, the use of more complex potential functions is not warranted at this stage of the study. This thus constitutes an informal proof of the assumption in this case. Hence, it may be stated that the energy coupling hypothesis can be used safely for vibrational transitions following the quantum harmonic oscillator model.

2.4   Spectroscopy

The use of spectroscopy provides an important mean to determine the structure of molecules. The most active region for vibrational modes is the infrared part of the spectrum. The individual frequencies are linked to given modes of individual bonds and quite extensively tabulated in the literature. Tabulated frequencies are usually given as an interval in order to account for the minor differences caused by the structure of each molecule (Mayo et al., 2004). In order to correctly interpret the molecular spectra and analyze spectroscopic data, vibrational, rotational and electronic modes must be taken into account. Although several tools such as the infrared and Raman spectrometer are used to study the infrared and near-infrared part of the spectrum, the fundamental principles exposed here are valid in the majority of cases.

The spectrometer, or more precisely the spectrophotometer, is the instrument used to study the atomic and molecular modes. This instrument consists basically of a light source, an optical wavelength separator (a prism or a diffraction grating), a cell containing the sample, and a detector. Figure 2.2 shows a simplified schematic of a spectrophotometer. Depending on the wavelength to be studied, the apparatus may use an infrared, ultraviolet or visible light source with an appropriate detector for the wavelength range. In the case of rotational and vibrational modes spectroscopy two methods are used: infrared absorption and Raman

Detector B (Raman)

Scattered light

Transmitted light

Source   Grating   Sample   Detector A (IR)
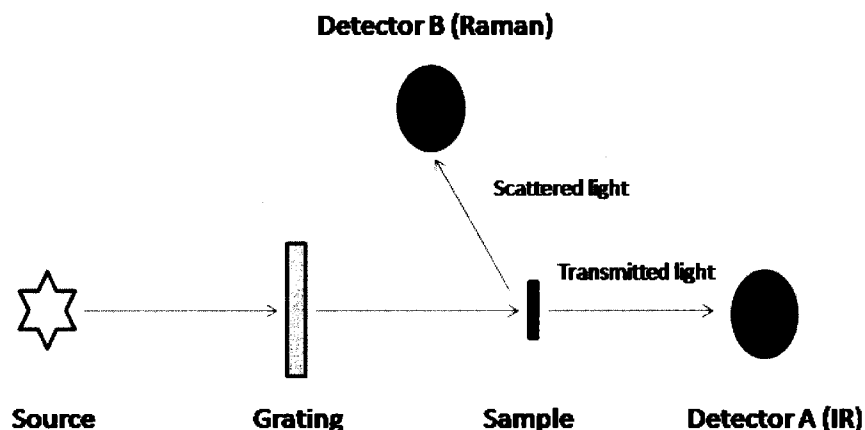
Figure 2.2. Simplified schematic of a spectrophotometer

scattering. In the infrared case, the incoming light is passed through the sample and the wavelength corresponding to the energy of a mode is absorbed. For Raman spectroscopy, a part of the incoming light is scattered (or reflected) by the material. This scattering can be imaged by the collision between a photon and a molecule. Some of the collisions are inelastic due to energy being transferred to the molecular modes. The energy difference between the incoming and the scattered photon will be the transferred energy and will correspond to a mode. The two detector configurations shown on figure 2.2 represent the infrared and Raman configurations. The data obtained on a spectrometer will consists of absorbances (or scattering) intensity with respect to wavelength. In the infrared and Raman cases, wavenumbers in units of cm^{-1} are used instead of wavelengths units. The conversion relations between wavenumber, wavelength and frequency are the following:

$$\lambda = 1/k \tag{2.4}$$

$$\nu = c/\lambda \tag{2.5}$$

where λ is the wavelength, k is the wavenumber in cm^{-1}, ν is the frequency in Hz, and c is the speed of light constant (3×10^8 m/s). In the case of visible and ultraviolet spectroscopy, wavelengths in units of nanometres or Angstroms are used as they are convenient in that particular range.

The vibrational energy levels of the simple linear molecule modelled by the quantum harmonic oscillator were given previously in equations 2.2 and 2.3. It is important to note that the set of possible state changes is called a selection rule and the change from ground state to $n_v = 1$ is the fundamental transition. Ideally, the selection rule for the vibrational quantum number n_v is $\Delta n_v = \pm 1, \pm 2, \pm 3$, etc. This causes spectral lines to be equally spaced on either side of the main line. The lines that represent the $\Delta n_v = \pm 2, \pm 3$, etc. transitions are called overtones. The anharmonious behaviour of molecular vibrational modes gives rise to the Morse potential curve and accounts for molecular dissociation (Laidler et al., 1982). However, for reasons stated before, the quantum harmonic oscillator shall be used here.

A closer observation of a vibrational spectral line shows that it is sometime actually made of finely spaced lines with decreasing amplitude. This is explained by the presence of rotational modes and their coupling with vibrational modes (Allen and Pritchard, 1974). Such a rotational behaviour will be present in gases and liquids as solids do not allow for rotational degrees of freedom. Rotational behaviour of molecules is modelled using the quantized classical rigid rotor example. The results are energy levels of value

$$E_J = h^2 J(J + 1)/8\pi^2 I \tag{2.6}$$

where I is the moment of inertia of the molecule, J is the rotational quantum number and h is the Planck constant (Pilar, 2001). The only transitions allowed are those with $\Delta J = \pm 1$ (selection rule). Graphically, this yields equally and finely spaced lines in the spectrum representing the different transitions possible. The line group above the central vibrational frequency corresponds to the $\Delta J = +1$ transition and is called the **R** branch while the remaining group is denoted as the **P** branch (note that there is no line at the central frequency as $\Delta J = 0$ is not permitted). Since different vibrational states have different bond length, the spacing between the lines on either side of the central frequency is variable because of the change in moment of inertia and its effect on rotation. Indeed the **P** branch lines spread out while the **R** branch lines get closer together (Allen and Pritchard, 1974). It is important to note that the fine spacing between rotational lines is of the order of 10-20 cm^{-1}. Therefore, many spectrometers are not precise enough to reveal this fine structure. Most spectra will therefore not show the rotational behaviour and each peak will be assigned to a particular
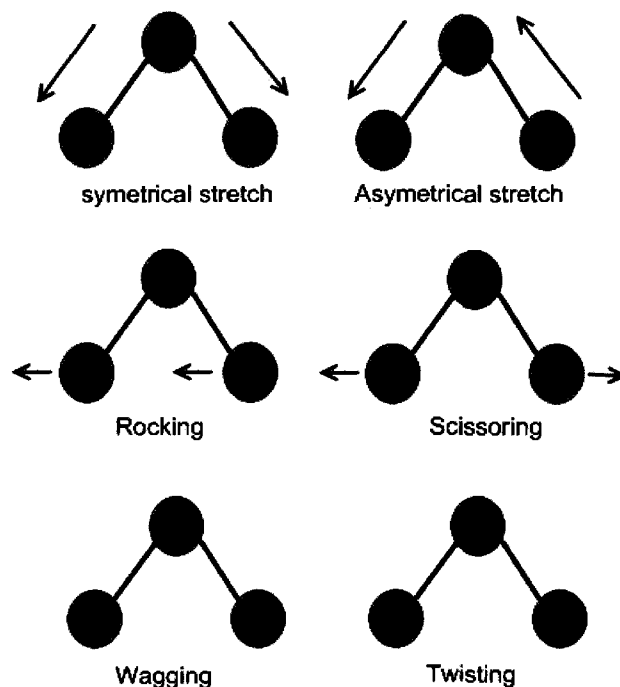
Figure 2.3. Representation of the different forms of vibrational modes

vibrational mode. It is however important to keep in mind the possible presence of rotational behaviour as these modes will absorb some energy.

In the case of the more complex polyatomic molecules such as those of value for this study, the same basic ideas apply. The most important difference arises from the multiplication of posible vibrational modes. The general rule for determining the number of modes of a molecule is as follows: given a molecule with n atoms, if it is a linear molecule, there are $3n-5$ vibrational modes, otherwise there are $3n - 6$ vibrational modes. The additional modes are due to the possible symmetric stretching, asymmetric stretching, bending, wagging, rocking and twisting in all planes of the individual bonds or groups, as shown on figure 2.3 for the case of H_2O (Laidler et al., 1982). Note that phenomena such as anharmonicity are also present in this case.

Electronic modes refer to the regions where electrons are located around an atomic nucleus. Such regions are the zones where there is a non negligible probability of having an electron present. The probabilities are computed using the wavefunction through solutions of the Schrodinger equation (Levine, 2005). The atomic system is often modelled as a finite potential well and the solutions for a single dimension are standing waves which integrally fit the "radius" of the orbit (note that these solutions are fully compatible with the energy coupling assumption). This wave-like behaviour is at the base of the famous wave-particle duality and was first proposed by DeBroglie (Pilar, 2001).

As discussed before, the energy function of an atomic bond usually has the form of the well known Morse potential. The curve shown on figure 2.1 represents a single electronic state. The different possible energies on the curve are quantized and these states are the different rotational and vibrational modes of the given electronic mode (Pilar, 2001). Hence a change in electronic state is represented as a jump to another curve of very similar shape with higher or lower energy. It can thus be seen that the absorption of an energy photon below a certain limit will increase the energy of the molecule through rotational and/or vibrational modes. Beyond the limit, an electronic transition (to another potential curve) will take place or the bond will break. Such an electronic transition can be accompanied or not by a rotational-vibrational transition. The determination of the final rotational-vibrational state during the electronic transition is made using the Frank-Condon principle which states that the overlap of the wave-functions of the initial and final state must be maximized (Levine, 2005).

Most electronic transitions starting from the ground state occur in the visible and ultraviolet part of the spectrum (wavelengths below 700 nm). This frequency range is scanned by a UV-visible spectrophotometer and the peaks observed can be linked to electronic transitions (Pavia et al., 2001). This particular data is important here as it sets a limit of validity due to the assumption requiring only vibrational dissociation. Therefore, the highest wavelength at which an electronic transition peak is located should be regarded as the smallest wavelength to consider when applying the energy coupling assumption.

It is now clearer how the global spectrum of energetic molecules should be studied in

order to perform the required calculations. The infrared spectrum contains the fundamental vibrational information of the ground electronic state of a molecule and the rotational modes are embedded in that spectrum as well (although often not discernable because of the precision required). The first electronic transitions are usually found in the higher energy part of the spectrum (often in the wavelengths around 200 nm) (McHale, 1999). This sets a limit on the multiple of the base vibrational frequencies that can be applied to get dissociation. Beyond this limit, the dissociation energy and the vibrational spectrum of the new electronic state (or Morse potential curve) will be required. The scope of this study is however to remain in the ground electronic state.

2.5 Molecular dissociation

The most important phenomenon studied in this work is molecular dissociation. The ways in which a bond can break are exposed here with respect to the previous discussions. Molecular dissociation occurs through vibrational or electronic excitation. When the vibrational energy of the bond is such that the rightmost part of the Morse potential curve is reached, the bond will break. The difference between the ground vibrational energy and the asymptotic value of the energy in a Morse potential function is defined as the dissociation energy on that given electronic level (or Morse curve) (Pilar, 2001). The dissociation energies values found in the literature all refer to the ground electronic state and are often obtained using spectroscopic measurements (as a difference between the excited species dissociation fragments excess energy and the electronic transition energy) (Barrow, 1966). It is important to note that the dissociation energies found in the literature usually only refer to the two direct members of the bond (for exemple a C-C bond alone that is not part of a larger molecule). In a larger molecule, the mechanics and forces of the system shall cause variations in these values. Hence, the use of literature dissociation energies here must be viewed as a simplification. In the case of dissociation through electronic excitation, an electron that receives a photon with energy large enough to escape the potential well or raise the electron to an antibonding orbital can cause the bond to break (Levine, 2005). The combination of both a vibrational

and an electronic transition can cause dissociation. The reason for such behaviour is found directly in the Frank-Condon principle. By this statement, it is well possible that in order for the wavefunctions of the initial and final states to have the maximum overlap, the final state will be in a different vibrational mode (McHale, 1999). The energy of the system could however be located on the asymptotic part of the new Morse curve and cause dissociation. Hence, although the dissociation is caused by the vibrational energy, the electronic transition is causing the shift to a vibrational mode where bond breaking becomes possible (Laidler et al., 1982). Again, it must be stressed that this study is confined to the case of dissociation through the sole vibrational excitation.

2.6   Summary

This chapter has laid the theoretical foundations on which the method is built. It is noted that the present study looks only at molecular dissociation due to the excitation of vibrational modes. The main assumption has been shown to be the energy coupling statement. The application of the energy coupling assumption has two major implications. The first one is of a more qualitative nature as it answers the question of how incoming energy will interact with the molecular system. The second implication is more quantitative and enables one to calculate the overtones of the fundamental vibrational frequency all the way to the dissociation limit. One must note that this last implication is dependant on the model used for the potential energy (the quantum harmonic oscillator and the Morse potential were looked at in this case). The choice of the quantum harmonic oscillator model here was purely based on the realisation that the added complexity of using the Morse potential in the calculations was not warranted by the slight increase in the precision of the final results. One must however note that if intermediate overtones are to be considered (the frequencies between the fundamental and the dissociation), the simple quantum harmonic oscillator should not be used as it will not be precise enough (an example would be the calculation of the vibrational partition function of a bond). The other assumptions are also important to the method but remain more straightforward.

It is useful to conclude this chapter by explicitly giving the steps required to apply the method developed. Upon reviewing the different steps, the importance of the assumptions used is easily seen. The method is given here in a list form:

1. Obtain the infrared and ultraviolet spectra information of the energetic molecule to be studied (this information can either be graphical or tabular peaks values)

2. From the knowledge of the different molecular bonds present (for example through a drawing of the molecule), use the literature data to assign bands wavelengths regions to specific bonds (textbooks on infrared spectroscopy usually contain numerous tables with such assignments).

3. Compare the data of steps 1 and 2 to assign absorption peaks to specific bonds.

4. Using literature values of the dissociation energies, the Planck's law is applied directly to find the exact dissociation frequencies (or wavelengths).

5. From the results of the two previous steps, calculate the exact quantum number value (not necessarily an integer) that will yield the dissociation frequency. Note that the quantum number value obtained should be rounded up to the next integer value to yield a result consistent with the energy coupling assumption in this case.

6. Calculate the frequency that matches the rounded value obtained in the last step. This frequency is the limit below which there will be no dissociation. A table of frequencies with respect to the quantum number can also be produced to show the progression of the overtones from the fundamentals to the dissociation limits.

Thus, it can be seen that the results of these calculation are data tables with fundamental and dissociation parameters (energies, frequencies, wavelengths, and quantum numbers). Each fundamental frequency in a table is linked with an actual mode directly in order to be able to further the analysis and predict which bond is subject to break first in a given case. The next chapter will apply the method presented here to the case of two widely used energetic molecules.

Chapter 3

Application of the Method

3.1 General overview

The last chapter presented the proposed method to study the initial condensed phase combustion reaction and established some basic ground rules to examine spectra of molecules in order to better predict the dissociation phenomena. In this chapter, the method and rules are applied to the cases of the following energetic materials: *nitroguanidine (NQ)* and *nitrocellulose (NC)*. The choice of these particular molecules is not arbitrary as they are not in the same family (a nitramine and a nitrate ester). In both cases, the analysis shall follow the same path with these given steps: infrared spectrum analysis, ultraviolet-visible spectrum analysis, applying the assumptions to calculate the limit wavelengths, and discussion on the results.

3.2 Example: Nitroguanidine

The vibrational modes of NQ can be obtained from the infrared spectrum on figure 3.1 (Sigma Aldrich catalog). The NQ spectrum shows several bands (or peaks) of absorption. It was shown that each band is centered at the vibrational mode frequency and that the thickness of the band is due to the rotational fine structure. It can be observed that more precision would

Figure 3.1. The infrared spectrum of nitroguanidine (Sigma Aldrich Catalog)

be required to show the detailed structure here. From figure 3.1, three separate zones can be noticed: one around 1500 cm^{-1}, one around 2900 cm^{-1}, and one last around 3300 cm^{-1}. It is not enough here to simply note the presence of a particular band. The peaks must be assigned to specific bonds in order for conclusions to be drawn from the calculation. This is done by consulting infrared spectroscopy group frequencies tables found in the literature. It is required here to be able to assign each band to a particular group bond in order to perform the dissociation calculation which comes after. When comparing a spectrum plot with actual individual bond data, it is important to keep in mind that there will be slight shifts in the frequencies due to the nature of what is attached on either side of the group which affects the mechanics of the oscillations (Mayo et al., 2004).

The nitroguanidine (NQ) molecule is shown on figure 3.2. This molecule contains elements of an aliphatic amine (R-NH$_2$) and an aliphatic nitrate (R-NO$_2$) together. The detailed spectroscopic data is presented as follows in a list form:

- The asymmetric and symmetric stretches of NH$_2$ are 3375 +/- 25 cm^{-1} and 3300 +/- 30 cm^{-1}, respectively (Pavia et al., 2001).

- The scissoring and wagging frequencies of NH$_2$ are respectively at 1620 +/- 30 cm^{-1}

30
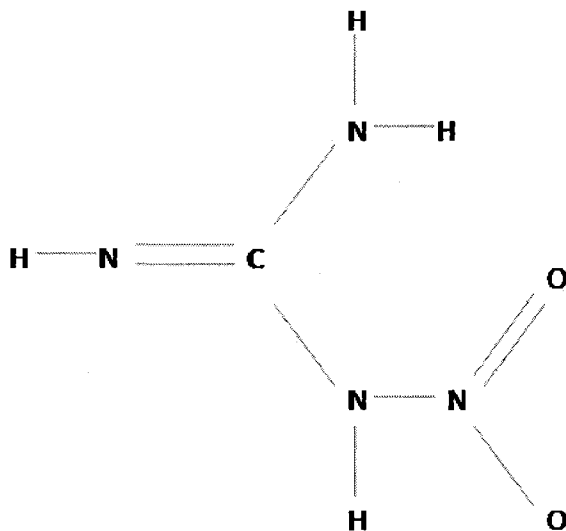
Figure 3.2. Schematic of the nitroguanidine molecule

and 800 cm^{-1} (Mayo et al., 2004).

- The N-H stretches are around 3400 cm^{-1} (Pavia et al., 2001).

- The C-N stretch is at 1665 +/- 25 cm^{-1} (Mayo et al., 2004).

- The asymmetric and symmetric stretches of NO_2 are 1531-1601 cm^{-1} and 1310-1381 cm^{-1}, respectively (Mayo et al., 2004).

- The in-plane bending, out-of-plane wagging and in-plane rocking frequencies of NO_2 are 610-660 cm^{-1}, 477-560 cm^{-1} and 470-495 cm^{-1}, respectively (Mayo et al., 2004).

- There are two close together bands around 2900 cm^{-1}. Literature shows clearly that such bands are usually the first to look for in an organic compound as they are the C-H stretching modes. NQ, however, does not contain any C-H bond. The hypothesis here is that the NQ could be in some organic solvent (Pavia et al., 2001). Hence these bands should be neglected in the analysis.

This covers most of the bands seen on figure 3.1. Note that given the location of the two band zones, overtones are normally expected to occur around 3000 cm^{-1} and 6000 cm^{-1}. Since overtones are of weaker intensities, they are not always observed and can be hidden by other bands. Hence some bands such as those in the higher frequency region (2500-3500 cm^{-1}) can be mixed with overtones. However this is not expected to modify the observation made above as the actual modes are stronger then the overtones. Two standalone bands that have not been discussed yet (around 1100 cm^{-1}) could indeed be overtones as well. The only question in this case is if the NQ sample was in another organic substance (such as a solvent) that could have created the two 2900 cm^{-1} bands. If so, then some of the not directly explained bands could also be possibly coming from this same substance.

The UV spectrum of NQ, given on figure 3.3, shows the electronic transitions frequencies (National Institute of Standards and Technologies). It is seen that there are two wavelengths (frequencies) of interest in this case (corresponding to maxima in the spectrum): 210 and 260 nm. Hence any wavelength close to or below these last two values should not be used to make any conclusion.

Based on the data presented previously, the dissociation wavelength can be computed using the method presented in chapter 2. The results of the dissociation calculations for NQ along with a compact list of the IR modes are shown on table 3.1. Note that the wavenumber values given are the central band values (maxima) on the actual spectrum of NQ and that the dissociation energies are from the literature (Franklin and Marshall College). It can be seen that the matching n values (frequency multiple to reach dissociation energy) are not integers. Since the permitted values of n are integers here, the first actual dissociation n values are the rounded up integer values. The set of possible wavelength between the fundamental and dissociation values have been tabulated and are shown in **Appendix A**. A graphical representation of this tabular data is shown on figure 3.4. Note that figure 3.4 is only an illustration of what would be observed and has not been generated by any calculations. The intermediate frequencies shown in figure 3.4 are coming from the use of both the quantum harmonic oscillator and the Morse potential.
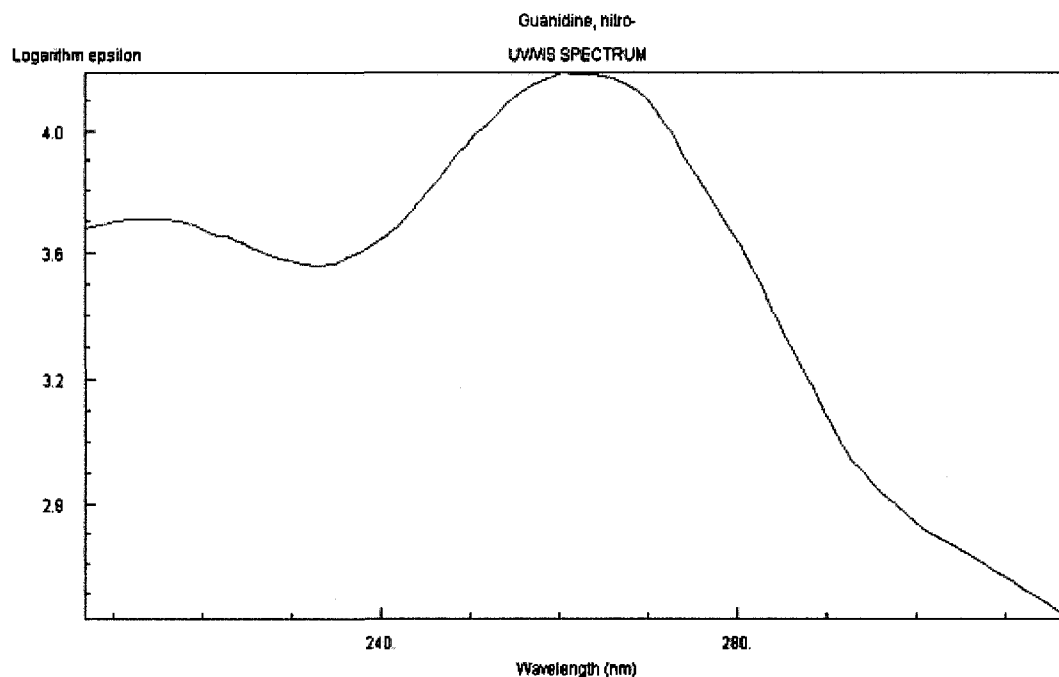
Figure 3.3. The ultraviolet spectrum of nitroguanidine

As an example, the full detailed calculation performed for the single bond NO_2 symetric stretch is shown below. Note that the step numbers used are the same as those presented at the end of chapter 2.

1. The IR and UV-visible spectra are shown on figures 3.1 and 3.3.

2. The assignment of band wavelength region is given in list format.

3. The assignment of absorption peaks to specific bond is shown on table 3.1. In the case of the NO_2 symetric stretch, the assigned wavenumber is 1300 cm^{-1}.

4. The dissociation energy for an N-O single bond can be found to be 2.3 eV. Using Planck's law $(E = h\nu)$, the following is obtained: $\nu = E/h$. Substituting for the energy value

Mode description	wavenumber	bond E	λ	frequency	n_v	n_v	limit λ	diss λ	$\Delta\lambda$
	(1/cm)	(eV)	(m)	(Hz)	match	exact	(nm)	(nm)	(nm)
NH_2 asym stretch	3350	4.01	3,0E-06	1.0E+14	9.6	10	310	299	11
NH_2 sym stretch	3270	4.01	3.1E-06	9.8E+13	9.9	10	310	306	4
NH_2 wagging	780	4.01	1.3E-06	2.3E+13	41.4	42	310	305	4
NH_2 scissoring	1630	4.01	6.1E-06	4.9E+13	19.8	20	310	307	3
NH stretch	3450	4.01	2.9E-06	1.0E+14	9.4	10	310	290	20
C=N stretch	1660	6.38	6.0E-06	5.0E+13	30.9	41	195	194	0
C-N stretch (NH2)	1050	3.17	9.5E-06	3.2E+13	24.3	25	392	381	11
C-N stretch (NO2)	1160	3.17	8.6E-06	3.5E+13	22.0	23	392	375	17
NO_2 sym stretch (N-O)	1300	2.3	7.7E-06	3.9E+13	14.2	15	540	513	27
NO_2 sym stretch (N=O)	1300	6.3	7.7E-06	3.9E+13	39.0	40	197	192	5
NO_2 asym stretch (N-O)	1530	2.3	6.5E-06	4.6E+13	12.1	13	540	503	37
NO_2 asym stretch (N=O)	1530	6.3	6.5E-06	4.6E+13	33.2	34	197	192	5
NO_2 rocking (in)	480	2.3	2.1E-05	1.4E+13	38.6	39	540	534	6
NO_2 wagging (out)	570	2.3	1.8E-05	1.7E+13	32.5	33	540	532	8
NO_2 bending (in)	650	2.3	1.5E-05	2.0E+13	28.5	29	540	531	9
N-N bond	NA	1.73	NA	4.18E+14	NA	NA	718	NA	NA

Table 3.1. Spectroscopy analysis and calculation results for nitroguanidine

given above and planck's constant in appropriate units (4.1×10^{-15} eV s), the follow-ing frequency is obtained: $\nu = 5.56 \times 10^{14}$ Hz. This last frequency corresponds to a wavelength of 540 nm (shown in table 3.1).

5. The fundamental frequency can be computed directly from the wavenumber value assigned in step 3: $\nu = c/\lambda$ where $\lambda = 1/k$ (here, k is the wavenumber). Using the velocity of light constant of 3×10^8 m/s, the value $\nu = 3.9 \times 10^{13}$ Hz is obtained. The exact dissociation quantum number is thus the ratio of the dissociation and the fundamental frequencies, which in this case yields 14.2. Hence the actual value of the first possible dissociation quantum number is the rounded up integer $n_v = 15$.

6. The first dissociation frequency value is then found from the following expression: $\nu_{diss} = n_v \nu_0$. This yield $\nu_{diss} = 5.85 \times 10^{14}$ Hz, which is equivalent to a wavelength of 513 nm (present in table 3.1).

It is interesting to compare the first dissociation wavelength of 513 nm with the limit value

34
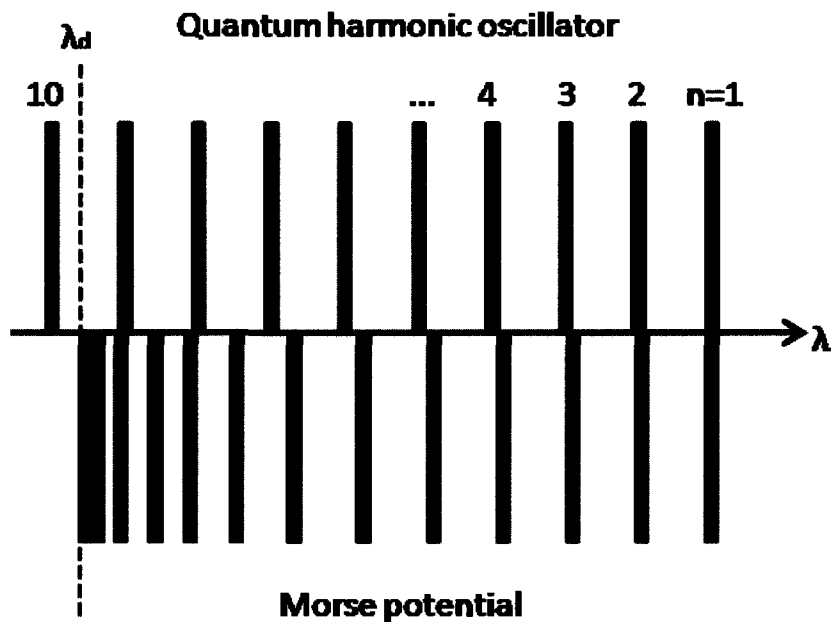
Figure 3.4. Graphical representation of appended tabular data for the NH_2 stretches

of 540 nm. This comparison enables to verify the actual difference between using the quantum harmonic oscillator and the Morse potential model (as the Morse potential model would yield the limit wavelength as the first dissociation value). This difference is of only 27 nm in this case, which is quite acceptable.

3.3 Example: Nitrocellulose

Nitrocellulose, shown on figure 3.5, is one of the most widely used energetic molecules and is the main ingredient of single base gun propellant. This compound is synthesized by nitrating cellulose, which is found in a variety of vegetal raw products (wood pulp and cotton are two important sources). The cellulose molecule is shown on figure 3.6. Upon nitration, the OH groups in cellulose are gradually replaced by $O-NO_2$ groups. The percentage of nitrogen present in the final product determines the grade of nitrocellulose. This is important in
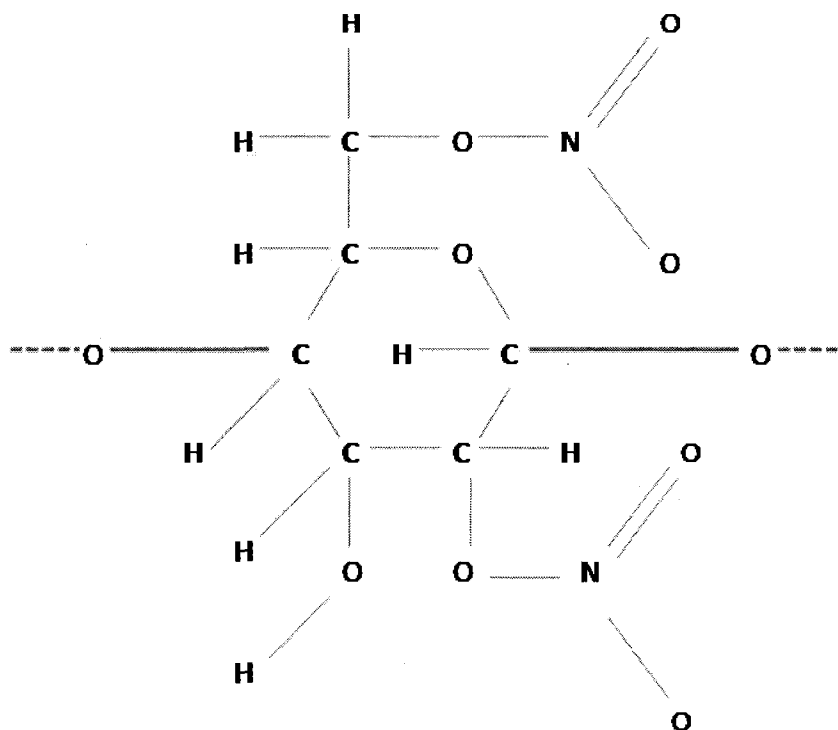
Figure 3.5. Schematic of the nitrocellulose molecule

applications as it has an impact on the energetic potential of the NC used. In the present case, the impact will be that OH group bands are to be expected depending on the grade of the NC represented in the infrared spectrum. It is important to note that NC consists of long chains of the cyclic group shown on figure 3.5 and connected through the lateral oxygen atom (two of these groups are represented on figure 3.5) (Akhavan, 1998).

The infrared spectrum peaks of nitrocellulose are given on table 3.2 and shown graphically in **Appendix B** (Giasson, 2005). Three main features can be observed in this spectrum: two standalone bands are present around 3000 cm^{-1}, the majority of the band are in the 1000-1500 cm^{-1} region and several scattered bands are seen under 1000 cm^{-1}. A literature review on the different groups and bonds present in the NC molecule yields the following information:

- The asymmetric and symmetric stretches of NO_2 are 1620-1640 cm^{-1} and 1270-1285
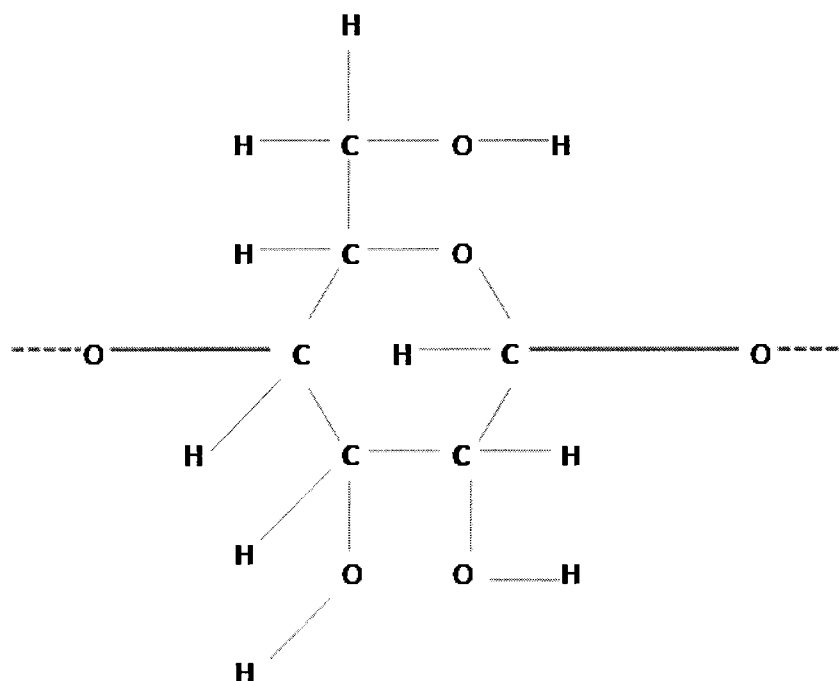
Figure 3.6. Schematic of the cellulose molecule

cm^{-1}, respectively (Mayo et al., 2004).

- The N-O stretch is in the interval 855-870 cm^{-1} (Mayo et al., 2004).

- The C-H stretch is located around 2700-3100 cm^{-1} (Pavia et al., 2001).

- The C-O stretch is located in the interval 1000-1300 cm^{-1} (Pavia et al., 2001).

- The in-plane bending and out-of-plane wagging are located in the intervals 755-760 cm^{-1} and 695-710 cm^{-1}, respectively (Pavia et al., 2001).

- The C-C bond stretches are very weak and will often mechanically couple. Hence, these cannot easily be observed and/or assigned.

All the modes described above have strong absorption and can easily be observed on the spectrum of table 3.2 (or in **Appendix B**). The detailed assignments are shown on table 3.3.

693 cm^{-1}	751 cm^{-1}	841 cm^{-1}	1004 cm^{-1}
1071 cm^{-1}	1162 cm^{-1}	1279 cm^{-1}	1377 cm^{-1}
1428 cm^{-1}	1652 cm^{-1}	2916 cm^{-1}	3573 cm^{-1}

Table 3.2. FT-IR spectroscopy peaks wavenumbers values

Mode description	wavenumber (1/cm)	bond E (eV)	λ (m)	frequency (Hz)	n_v match	n_v exact	limit λ (nm)	diss λ (nm)	$\Delta\lambda$ (nm)
O-H bond stretch	3573	4.76	2.8E-06	1.1E+14	10.7	11.0	261	254	6
C-H bond stretch	2916	4.26	3.4E-06	8.7E+13	11.8	12.0	292	286	6
C-O bond stretch	1071	3.71	9.3E-06	3.2E+13	27.9	28.0	335	333	1
C-C bond stretch	weak	3.59	NA	NA	NA	NA	346	NA	NA
N-O bond stretch	841	2.3	1.2E-05	2.5E+13	22.02	23.0	540	517	23
NO_2 sym stretch (N-O)	1279	2.3	7.8E-06	3.8E+13	14.5	15.0	540	521	19
NO_2 sym stretch (N=O)	1279	6.3	7.8E-06	3.8E+13	39.7	40.0	197	195	2
NO_2 asym stretch (N-O)	1652	2.3	6.1E-06	5.0E+13	11.2	12.0	540	504	36
NO_2 asym stretch (N=O)	1652	6.3	6.1E-06	5.0E+13	30.7	31.0	197	195	2
NO_2 bending (in)	751	2.3	1.3E-05	2.3E+13	24.7	25.0	540	533	7
NO_2 wagging (out)	693	2.3	1.4E-05	2.1E+13	26.7	27.0	540	534	6

Table 3.3. Spectroscopy analysis and calculation results for nitrocellulose

It was not possible to obtain the ultraviolet-visible spectrum of NC in a graphical format. A study by Gavrilov and Ermolenko published in 1967 was found where the main absorption values were given in the UV-visible spectrum of cellulose and cellulose derivatives (including nitrocellulose). From this study, it is clear that an absorption peak is present in the region around 200-240 nm for NC (Gavrilov et al., 1967). Hence, the limiting wavelength of validity should be taken as 240 nm in this case.

The full calculation results are shown on table 3.3. Note that that steps used here are exactly the same as those needed for nitroguanidine, hence a sample calculation is not required here. Note here that the difference between the limiting wavelength and the first dissociation value is again quite acceptable. Again the intermediate frequencies are tabulated in **Appendix A.**

Nitroguanidine dissociation wavelengths (nm)

Nitrocellulose dissociation wavelengths (nm)
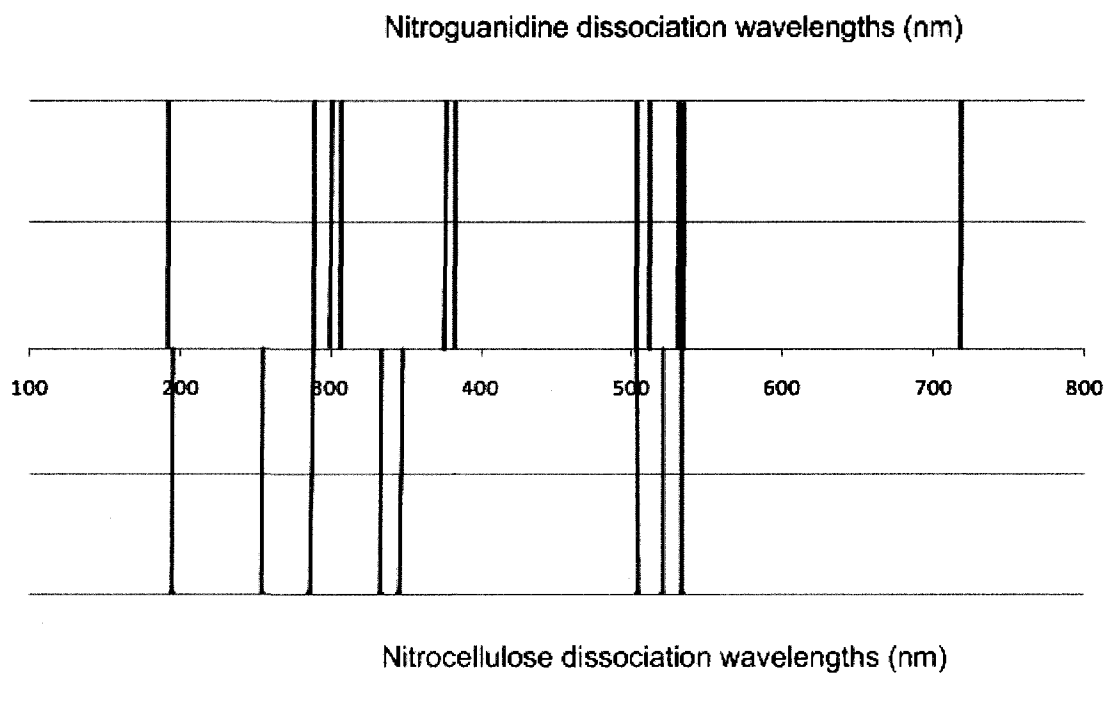
Figure 3.7. First dissociation wavelengths calculated for NQ and NC

3.4 Discussion on the calculations results

Interesting similarities arising from the presence of similar groups can be observed for both the nitrocellulose and the nitroguanidine case. Figure 3.7 shows a graphical representation of all the first dissociation wavelengths for both cases (the blue lines refer to NQ and the red lines to NC). The small differences that are observed between values of a same group arise from the differences in the fundamental frequencies. Thus those differences are caused by the different nature and geometry of each molecule. Another important fact to realize is that only small differences are observed between the dissociation wavelength calculated from both potential model (quantum harmonic oscillator and Morse potential). This would tend to show that going through the full spectral analysis is not warranted to attain the goals of this work. However, showing the smallness of this difference is important at this stage and

39

the failure to do so would have shown a lack of completeness. Furthermore, any continuation to this work leaning toward computing other combustion properties will require performing statistical mechanical calculations. Such calculations shall require the partition function to be known, thus requiring the fundamental modes to be known. Therefore for these reasons, it is necessary to go through the spectroscopic analysis step.

The main conclusion to make concerning these calculations is that the nitrate group (or NO_2 group) is the one that requires the minimum amount of energy to break and thus that would be most prone to begin a combustion reaction. However, to state that a group or another shall begin the reaction, the spectrum of the excitation energy must be examined as the quantum nature of the system will require very specific energy values in order to excite very specific bonds (or groups). The comparison of the results obtained in this chapter and the input energy spectra is the main subject of the following and last chapter of this thesis.

Chapter 4

Energy Input Spectrum and Ignition

4.1 General overview

The last two chapters focused on validating and showing how to use a simplified method that enables one to predict how input energy will couple to a given molecular bond and if dissociation is likely to occur. However, to be useful in practical applications, one additional step must be performed: comparing the spectrum of possible excitations with the spectrum of the incoming energy to find out if there are any matches. This last task is not as simple as it could seem as the source of this energy cannot be neglected in the evaluation. The subject of ignition thus becomes of importance in order to better characterize each type of source and apply the method developed in this work accordingly. This last chapter will first address this issue of ignition along with giving a list of possible energy sources. One such sources shall then be expanded on by using published emission spectroscopy data and the calculation examples of chapter 3 (nitroguanidine and nitrocellulose). A discussion follows on application with other input sources focusing on future research that could ensue from this work.

4.2   Ignition and some possible sources

Ignition is usually defined as the onset of the self-sustained reaction that is combustion (Meyer, 2003). Hence, the activation energy required to break the first bonds is exactly the ignition energy. Ignition has been described in most publications as mostly a thermal problem by opposition to a photodissociation issue (De Young, 1995; Babrauskas, 2003). However, the term "thermal", although pointing to the concepts of heat transfer and ignition temperature, is not a very precise one. In present modelling, the classical heat transfer theory is applied to simulate the temperature rise to the ignition temperature where the combustion chemistry is added into the analysis (Beckstead, 2006). It is however interesting to note that concepts such as temperature and heat transfer actually represent deeper molecular issues.

- Temperature is recognised as the measure of the total energy contained in the molecular system, which generally consists of the translational, rotational and vibrational energies (Hill, 1987).

- Heat transfer has three modes; conduction, convection and radiation. Conduction directly involves the spreading of vibrational motion through a solid substance. Radiation consists of transfer through electromagnetic energy, or photons (Holman, 2001).

Thus it is seen that although the term thermal is used, there is a deeper implication with the molecular structure and dynamics that has been covered all through this study. From the above considerations, ignition can thus be more precisely described as an excitation of certain molecular vibrational, translational or electronic modes causing the rupture of their corresponding bonds. It is then natural to realize that understanding a given energy input mechanism becomes important in the analysis. Several such mechanism relevant to propellant combustion are listed here:

- *Temperature*: In this case, the temperature is viewed as the sole source of molecular excitation. In the case of solids, only vibrational modes are involved. It is important

in this case to well understand phenomena involved in changing the temperature of a sample (interactions). The simplest case would be to consider different steady state temperatures without any external stimulus that would cause variation. Such a problem is beyond the scope of this work but would be an interesting continuation.

- *Photodissociation*: This simple case considers a photon being absorbed by a given bond that would excite the bond to a dissociation vibrational energy level. It is obvious to observe that this case can be easily applied to the method developed in this research.

This last case presented shall be the one expanded in this chapter. In order to obtain the correct input energy spectrum, more must be known about the source itself. In the case of propellant combustion, this source is most often either the combustion of an initiating compound (such as the well known black powder) or the combustion of the propellant itself (in a chain reaction where part of the energy liberated by the decomposition of the material goes back into providing the activation energy to more of the material). The first source thus usually governs the beginning of the combustion and the second will guide what remains. The next section will look at these different sources through some examples.

4.3   Input spectrum through emission spectroscopy

The spectroscopic data collected from analyzing the light emitted during combustion is usually referred to as an emission spectrum (as opposed to the absorption spectra that were reviewed before). Emission spectra are usually studied to determine the combustion products during a given reaction as different radicals will exhibit certain frequency bands only. It thus becomes interesting to compare the dissociation wavelengths of a given energetic molecule and the emission spectrum of any of the substance present in the combustion. As stated previously, in this case the two substances likely to be present will be the igniter composition (such as black powder) and the main energetic molecule. For one to predict the initial reaction, it then becomes a matter of determining by inspection which ignition wavelengths are embedded in emission regions.
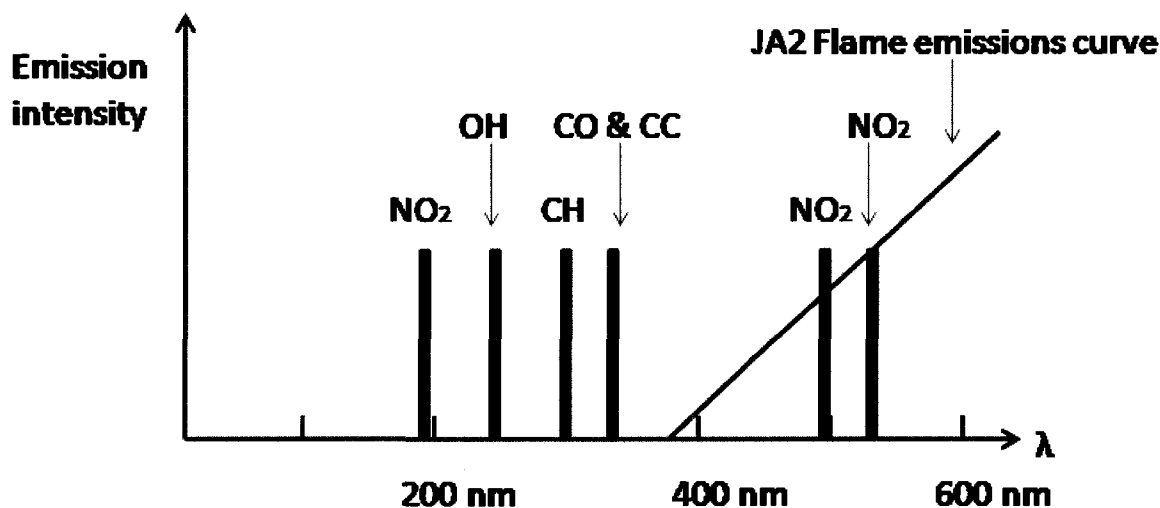
Figure 4.1. Comparison of dissociation wavelengths of NC with the emission spectrum for JA2

As an example, emission spectra in the visible-UV region of propellants containing ingredients discussed in chapter 3 can be studied. For the purpose of this work, the emission spectrum of JA2 propellant is a good first example. The energetic ingredients contained in JA2 are the nitrate esters nitrocellulose, nitroglycerin, and diethylene glycol dinitrate. The emission spectrum curve of JA2 begins rising from an intensity of zero at about 375 nm and has a fairly linear rise (Eisenreich et al., 2000). Plotting this with the nitrocellulose dissociation wavelengths (by drawing vertical bars at bond breaking values) enables the comparison leading to a prediction to be made (see figure 4.1). Observing figure 4.1 enables one to quickly determine that the NO_2 groups of the NC molecule shall be the first to secede as they are the only with dissociation wavelengths high enough to be in the region of emission. Upon absorption of the photonic emission of burning JA2 propellant, NC (as shown in figure 3.5 with the main cycle shown having x repetitions) will initially decompose as follows according to the model developed in this work:

$$\text{NC } (C_6H_8N_2O_9)_x = (C_6H_8O_5)_x + (2NO_2)_x \tag{R-7}$$

It is interesting to look at other combustion emission spectra from other energetic materials

44
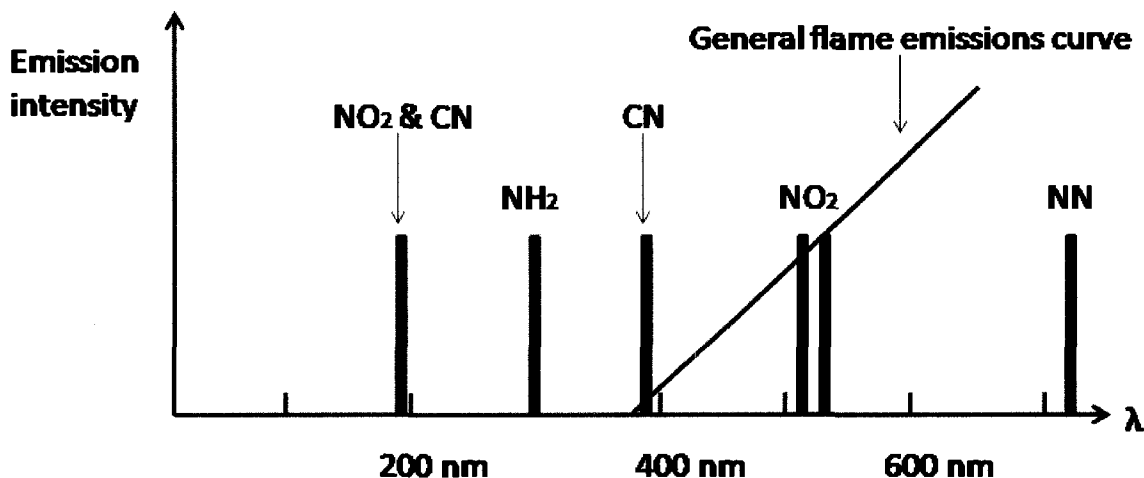
Figure 4.2. Comparison of dissociation wavelengths of NQ with the general emission spectrum trend

as some similarities can be observed. More precisely, the emission spectra from an RDX propellant (Weiser et al., 1999) and pyrotechnic compositions (Gillard et al., 2002) were studied. The quasi-linear increase from a zero intensity starting at wavelengths in the range 350-450 nm can quite often be observed. This seems to indicate that emissions in the ultraviolet range are not common in combustion phenomena. Hence the first reaction derived for NC can be reasonably expected not to change. Furthermore if the same analysis is applied to NQ, the initial reaction derived is the following:

$$CH_4N_4O_2(\text{nitroguanidine}) = HCN + NH_2 + NH + NO_2 \qquad \text{(R-8)}$$

It can be noted that this last reaction is exactly the same as reaction R-2 given in the first chapter when discussing the condensed phase reactions of energetic molecules families. The graphical representation of the analysis for NQ is shown on figure 4.2.

The application of the results obtained in the method developed in this work to combustion emission spectroscopy has shown here to yield results that are aligned with the current ideas about initial reactions for the case of nitrocellulose and nitroguanidine (a nitrate ester and a nitramine with different groups). This was however a very simple way to rapidly apply the

results in order to get meaningful information. It is obvious that other sources must also be studied for completeness. The following section introduces another such source along with some intricacies brought about by considering this source.

4.4   Ignition through a temperature rise

Certain points must however be put forward in order to better analyze the present case. From the observation of the spectroscopic analysis results, it can be noticed that the limit wavelengths are all in the visible and ultraviolet range (i.e. in the range between 200 nm and 700 nm). Since these wavelengths are within the range of ambient light, it can be concluded that these dissociation reactions should be occurring constantly under normal conditions. This is indeed the case and that situation is a major product safety concern for propellant designers (short and long term propellant stability) (Urbanski, 1984). In the case of widely used energetic substances, these decomposition reactions are occurring at a fairly slow rate but the decomposition products increase the acidity of the surroundings which gradually causes an augmentation of the reaction rate. Because of this feedback effect, the substance can reach a state where the reaction rate will jump up and a fast combustion will occur. This jumping point that separates the regime in which the material exists in a relatively stable form and that in which a violent reaction occurs is of course what is normally referred to as the ignition point (Kubota, 2007). From a statistical mechanics standpoint, there should be an important increase of the number of bonds with an energy equal or grater then what is required for dissociation at the point of ignition. It is interesting to realize that the phenomenon is merely a rate increase of something that is already occurring. Hence the conclusion is that ignition has to do with the kinetics of the process. Kinetics is, however, beyond the scope of the present work but should be viewed as a necessary step in order to examine other sources, such as temperature, in detail.

In the case of a solid, temperature is a measure of the total vibrational energy contained in the system (Hill, 1987). Through statistical mechanics, the distribution of vibrational energy

46
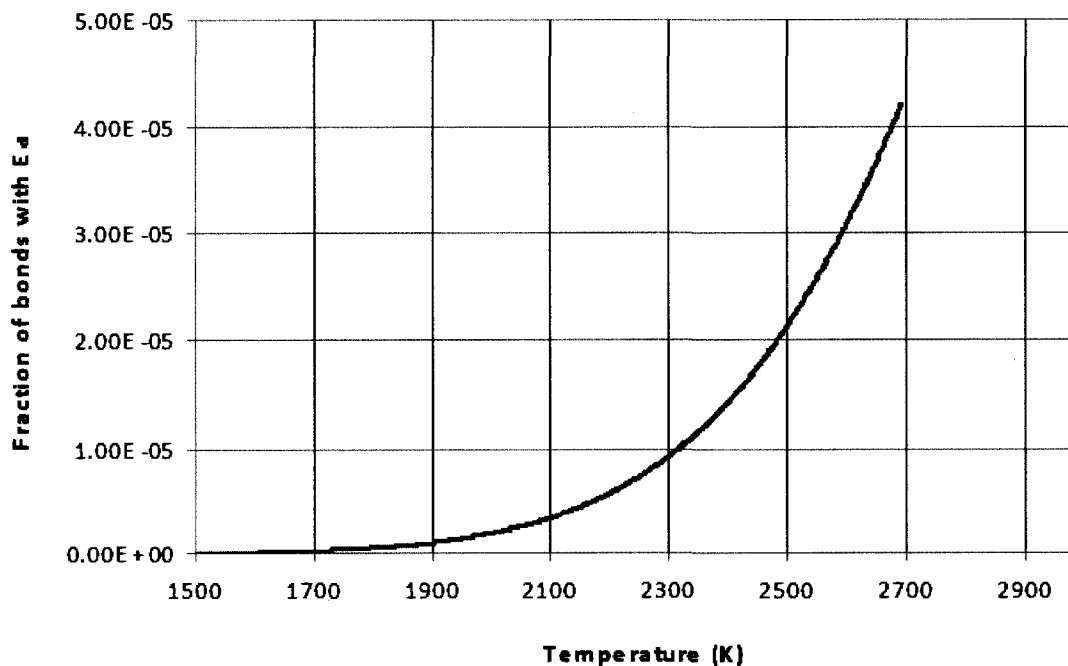
Figure 4.3. Fraction of bonds with the dissociation energy (NO_2 stretches case)

levels can be calculated. The general expression used to calculate the percentage of units at a given state with temperature is the following:

$$f(T) = \frac{e^{-E_d/k_bT}}{Z} \tag{4.1}$$

where Z is the famous partition function (or sum-over-all-states function) and is defined as follows:

$$Z = \sum_{n=0}^{\infty} e^{-E_n/k_bT} \tag{4.2}$$

In order to correctly evaluate Z, the values of energies must be known as precisely as possible (Hill, 1987). A correct model is required for this task. As discussed in chapter 2, there are several such models available but the Morse potential function is more precise than the quantum harmonic oscillator used for the method developed here. Hence the partition function should be calculated with energy values obtained from applying the Morse expression

47

(Laidler, 1982). Using the simple quantum harmonic oscillator model, the following partition function is obtained:

$$Z = \frac{e^{-h\upsilon_0/2k_bT}}{1 - e^{-h\upsilon_0/k_bT}} \tag{4.3}$$

Applying this function to the percentage of units expression yields the distributions shown on figure 4.3. The kinetic behaviour that is responsible for ignition can be observed on figure 4.3 as an abrupt increase in the number units with sufficient energy for dissociation. With an appropriate choice of the temperature value where the change of slope occurs, one can determine a possible ignition temperature for the given case. However, the temperature values that would be obtained with the case shown on figure 4.3 (around 2000 K) are not at all close to known experimental ignition temperatures values (usually closer to 500-600 K for typical energetic materials used for propellants). Hence, the model does not yield good results as expected and the more precise Morse potential should be applied. This opens a new direction and should be a direct next step in this line of research.

Chapter 5

Conlusions

5.1 Concluding remarks

From the results obtained in the different calculations and comparison made in this study, the original assumption and ideas leading to the methodology chosen have been validated as they corroborate well with the current ideas found in the literature. An important part of this study was to perform a large literature review to assemble the different main ideas relevant to condensed phase combustion and gasification combustion reactions. The elaboration and proof of the different steps in the method along with the spectroscopic analysis of the two examples has enabled to gather important information that will be useful in continuing this research. That last achievement was an important goal of the present work as it was known prior to the beginning that it would be an introduction to this type of simplified reasoning applied to condensed phase combustion.

The main question that was invoked in the introduction was about the correct coupling of energy with molecular systems. This question was answered mainly through the use of potential energy models but the choice of model was shown to be dependant on the context of the problem (Laidler, 1982). More precisely, the general method yielding dissociation wavelengths was shown to be of acceptable precision with the simple quantum harmonic

oscillator while any calculation requiring intermediate frequencies needs a more precise model (such as the Morse potential). In addition, molecular systems in their ground electronic states were assumed throughout the calculations as a first simplification.

The application of the method with the assumption of bond breaking solely through photodissociation using emission spectroscopy has yielded results quite in agreement with current theories regarding initial gasification reactions. The initial reactions for both nitroguanidine and nitrocellulose were given explicitly. It is however obvious that temperature has an important role to play in the later stage of the reaction but the assumption of photodissociation seems reasonable at the early stage studied here. An important task to perform will be to gather more emission spectroscopy data for the common cases (black powder ignition, standard propellant, energetic molecules) to verify that there are no anomalies. This last task coupled with applying the method with more molecules from different families will help in ensuring that the method is generally valid. The ultimate engineering goal would be to find an ingredient that would have photonic combustion emissions differing from those observed in this study in order to modify the initial reaction in a precise fashion (and possibly modify the propellant burning rate as well).

It was shown that there are many possible continuations to this research. The most obvious is the application of statistical mechanics principles to accurately predict the run-up point of the temperature distribution curve for different bonds and determine the ignition temperature. This will be more complex due to the calculations involved but the spectroscopic data obtained from the analysis shall be essential in performing the analysis. Another important sequel would be to obtain the pyrolysis law parameters (see equation 1.1 in chapter 1) through calculations using the principles introduced here. This again would involve statistical mechanics as kinetics is involved in deriving a reaction rate law. There would also be other, more applied, studies such as other ignition sources like laser, electric discharge, plasma, and shock interaction with an energetic molecule.

Following the additional verifications discussed above, the method should be applied to a current propellant burning rate prediction algorithm in order to have a complete tool that

would not require a guessing step (Miller and Anderson, 2004). This is important as it was through the review of literature pertaining to this subject that came the original idea for pursuing the research done here. To conclude, the goals of defining a way in which the energy couples to an energetic molecule, acquiring molecular modal data through spectroscopy, and predicting an initial reaction to the combustion of a given energetic molecule were attained with success. The first results obtained are in agreement with currently published ideas. Hence, through gathering additional data to reinforce the conclusions and pursuing the research in the areas mentioned previously, the empirical methodology introduced here shall be more completely validated. This will contribute in increasing our understanding in condensed phase combustion and shall enable designers to successfully come up with new and efficient applications.

5.2   Contribution to knowledge

Throughout the initial chapter of this thesis, it was stressed that current methods used to study condensed phase combustion require very complex computations that render the whole analysis expansive and inefficient. It was the main goal of this work to lay the foundations of a simplified methodology through theoretical considerations and empirical measurements. These measurements are mainly made through absorption and emission spectroscopy. Care was taken in verifying the simplification steps and assumptions through basic quantum mechanics. The two examples used showed that the methodology leads to predictions that are within the current thoughts about gasification reactions. The tools gathered in this thesis can now be readily applied with statistical mechanics in order to cover the kinetics aspect and thus have a more complete picture of the condensed phase combustion phenomena. The results obtained along with those already available from the conclusion of this work shall prove useful in designing more complete combustion modeling tools.

References

[1] Akhavan, J. (1998) *The Chemistry of Explosives*. Royal Society of Chemistry.

[2] Allen, G. and Pritchard, H.O. (1974) *Statistical Mechanics and Spectroscopy*. Halsted.

[3] Babrauskas, V. (2003) *Ignition Handbook*. Fire Science Publishers.

[4] Barrow, G.M. (1966) *Physical Chemistry*. McGraw-Hill.

[5] Beckstead, M. W. (2006) Recent progress in modeling solid propellant combustion. *Combust., Expl. Shock Waves* **42 (6)**, pp. 623-641.

[6] Beyer, R.A. and Pesce-Rodriguez, R.A. (2004) The response of propellants to plasma radiation. *Proc. 12th symposium on Electromagnetic Launch Technologies*.

[7] De Yong, L., Nguyen, T. and Waschl, J. (1995) Laser ignition of explosives, pyrotechnics and propellants: A review, *DSTO Internal Report*, DSTO-TR-0068.

[8] Dlott, D.D. (2003) Fast molecular processes in energetic materials. *Theoretical and Computational Chemistry; Energetic Materials – Part 2: Detonation and Combustion,* pp. 125-192.

[9] Eisenreich, N., Eckl, W., Fisher, T., Weiser, V., Kelzenberg, S., Langer, G. and Baier, A. (2000) Burning phenomena of the gun propellant JA2. *Propellants, Explosives and Pyrotechnics* **25**, pp. 143-148.

[10] Franklin and Marshall College, Lancaster, PA. website: http://wulfenite.fandm.edu.

[11] Gavrilov, M.Z. and Ermolenko, I.N. (1967) Electronic absorption spectra of some cellulose derivatives. *Zhurnal Prikladnoi Spektroskopii* **6** (6), pp. 754-758.

[12] Giasson, G. (2005) FT-IR measurement curve on nitrocellulose. *Technical Report*, General Dynamics – Ordinance and Tactical systems Canada – Valleyfield.

[13] Gillard, P., De Izarra, C. and Roux, M. (2002) Study of the radiation emitted during the combustion of pyrotechnics charges. Part II: characterization by fast visualization and spectroscopic measurements. *Propellants, Explosives and Pyrotechnics* **27**, pp. 80-87.

References

[14] Hill, T.L. (1987) *An Introduction to Statistical Thermodynamics*. Dover Publications.

[15] Holman, J.P. (2001) *Heat Transfer*. 9th edition, McGraw Hill.

[16] Kee, R.J., Grear, J.F., Smooke, M.D. and Miller, J.A. (1985) A Fortran program for modelling steady laminar one-dimensional premixed flames. *Sandia National Laboratory Report* SAND85-8240.

[17] Korobeinichev, O. (2000) Flame structure of solid propellants. *Prog. Astro. Aero.* **185**, pp. 335-354.

[18] Kubota, N.(2007) *Propellants and Explosives − Thermochemical Aspects of Combustion*. 2nd Edition, Wiley-VCH.

[19] Kubota, N. and Sakamoto, S. (1989) Combustion mechanism of HMX. *Propellants, Explosives, Pyrotechnics* **14**, pp. 6-11.

[20] Kubota, N. and Sonobe, T. (1988) Combustion mechanism of azide polymer. *Propellants, Explosives, Pyrotechnics* **13**, pp. 172-177.

[21] Kubota, N., Hirata, N. and Sakamoto, S. (1988) Decomposition chemistry of TAGN. *Propellants, Explosives, Pyrotechnics* **13**, pp. 65-68.

[22] Laidler, K.J. and Meiser, J.H.(1982) *Physical Chemistry*. Benjamin Cummings.

[23] Levine, R.D.(2005) *Molecular Reaction Dynamics*. Cambridge University Press.

[24] Liau, Y.C., Yang, V. (1995) Analysis of RDX monopropellant combustion with two-phase subsurface reactions. *J. Propulsion Power* **11**, pp. 729-739.

[25] Mayo, W.M., Miller, F.A. and Hannah, R.W. (2004) *Course Notes on the Interpretation of Infrared and Raman Spectra*. Wiley-Interscience.

[26] McHale, J.L. (1999) *Molecular Spectroscopy*. Prentice Hall.

[27] Meyer, R. (1981) *Explosives*. 2nd edition, Verlag Chemie.

[28] Miller, M.A. and Anderson, W.R. (2000) Energetic material combustion modeling with elementary gas-phase reaction: A practical approach, *Prog. Astronaut. Aero* **185**, pp. 501-531.

[29] Miller, M.A., Anderson, W.R .(2004) A practical approach to the theoretical prediction of propellant burning rate. *J. Propulsion Power* **20**, pp. 440.

[30] Miller, M.A., Anderson, W.R. (2004) Model for combustion of triple-base propellant with detailed chemistry. *Proc. of the 24th Army Science Conference*, Orlando, FL, Nov, 2004.

[31] MURI group webpage: http://chem.missouri.edu/Thompson/MURI02/

References

[32] National Institute of Standards and Technologies website: http://webbook.nist.gov

[33] Pavia, D.L., Lampman, G.M. and Kriz, G.S. (2001) *Introduction to Spectroscopy.* 3rd edition, Brooks & Cole.

[34] Pilar, F.L. (2001) *Elementary Quantum Chemistry.* Dover Publications.

[35] Schroeder, M.A., Fifer, R.A., Miller, R.A., et al. (2001) Condensed-phase processes during combustion of solid gun propellants; I-Nitrate Ester propellants. *Combust. Flame* **216**, pp. 1569-1576.

[36] Sigma Aldrich Catalog: http://www.sigmaaldrich.com

[37] Sorescu, D.C., Rice, B.M. and Thompson, D.L. (2003) Molecular dynamics simulations of energetic materials. *Theoretical Comput. Chemistry, Energetic Materials Part 1: Decomposition, Crystal and Molecular Properties*, pp. 125-184.

[38] Urbanski, T. (1967) *The Chemistry and Technology of Explosives.* Pergamon Press.

[39] Volk, F. (1985) Determination of gaseous and solid decomposition products of nitroguanidine. *Propellants, Explosives, Pyrotechnics* **10**, pp. 139-146.

[40] Weiser, V., Eisenreich, N. and Eckl, W. (1999) *From Rocket Exhaust Plume to Fire Hazards – Methods to Analyze Radiative Heat Flux, Prevention of Hazardous Fires and Explosions.* NATO Science Series, Springer.

[41] Zenin, A.(1995) HMX and RDX: Combustion mechanism and influence on mModern double base combustion. *J. Propulsion Power* **11**, pp. 752-758

Appendices

Appendix A – Tabulated data of nitroguanidine example calculation

matching n_d	9,6	9,9	41,4	19,8	9,4	30,9	24,3	22,0
diss λ (nm)	298,5	305,8	305,3	306,7	289,9	194,3	396,8	374,8
wavenumber (1/cm)	3350	3270	780	1630	3450	1660	1050	1160
fundamental λ (m)	2,985E-06	3,058E-06	1,282E-05	6,135E-06	2,899E-06	6,024E-06	9,524E-06	8,621E-06
n	**λ (nm)** ...							
1	2985	3058	12821	6135	2899	6024	9524	8621
2	1493	1529	6410	3067	1449	3012	4762	4310
3	995	1019	4274	2045	966	2008	3175	2874
4	746	765	3205	1534	725	1506	2381	2155
5	597	612	2564	1227	580	1205	1905	1724
6	498	510	2137	1022	483	1004	1587	1437
7	426	437	1832	876	414	861	1361	1232
8	373	382	1603	767	362	753	1190	1078
9	332	340	1425	682	322	669	1058	958
10	299	306	1282	613	290	602	952	862
11	271	278	1166	558	264	548	866	784
12	249	255	1068	511	242	502	794	718
13	230	235	986	472	223	463	733	663
14	213	218	916	438	207	430	680	616
15	199	204	855	409	193	402	635	575
16	187	191	801	383	181	377	595	539
17	176	180	754	361	171	354	560	507
18	166	170	712	341	161	335	529	479
19	157	161	675	323	153	317	501	454
20	149	153	641	307	145	301	476	431
21	142	146	611	292	138	287	454	411
22	136	139	583	279	132	274	433	392
23	130	133	557	267	126	262	414	375
24	124	127	534	256	121	251	397	359
25	119	122	513	245	116	241	381	345
26	115	118	493	236	111	232	366	332
27	111	113	475	227	107	223	353	319
28	107	109	458	219	104	215	340	308
29	103	105	442	212	100	208	328	297
30	100	102	427	204	97	201	317	287

Appendix A – continued

matching n_d	14,2	39,0	12,1	33,2	38,6	32,5	28,5
diss λ (nm)	512,8	192,3	502,8	192,2	534,2	531,6	530,5
wavenumber (1/cm)	1300	1300	1530	1530	480	570	650
fundamental λ (m)	7,692E-06	7,692E-06	6,536E-06	6,536E-06	2,083E-05	1,754E-05	1,538E-05
n	λ (nm)	...					
1	7692	7692	6536	6536	20833	17544	15385
2	3846	3846	3268	3268	10417	8772	7692
3	2564	2564	2179	2179	6944	5848	5128
4	1923	1923	1634	1634	5208	4386	3846
5	1538	1538	1307	1307	4167	3509	3077
6	1282	1282	1089	1089	3472	2924	2564
7	1099	1099	934	934	2976	2506	2198
8	962	962	817	817	2604	2193	1923
9	855	855	726	726	2315	1949	1709
10	769	769	654	654	2083	1754	1538
11	699	699	594	594	1894	1595	1399
12	641	641	545	545	1736	1462	1282
13	592	592	503	503	1603	1350	1183
14	549	549	467	467	1488	1253	1099
15	513	513	436	436	1389	1170	1026
16	481	481	408	408	1302	1096	962
17	452	452	384	384	1225	1032	905
18	427	427	363	363	1157	975	855
19	405	405	344	344	1096	923	810
20	385	385	327	327	1042	877	769
21	366	366	311	311	992	835	733
22	350	350	297	297	947	797	699
23	334	334	284	284	906	763	669
24	321	321	272	272	868	731	641
25	308	308	261	261	833	702	615
26	296	296	251	251	801	675	592
27	285	285	242	242	772	650	570
28	275	275	233	233	744	627	549
29	265	265	225	225	718	605	531
30	256	256	218	218	694	585	513

Appendix A – Tabulated data of nitrocellulose example calculation

matching n_d	10,7	11,8	27,9	NA	30,3	14,5
diss λ (nm)	260,9	291,5	334,8	346,0	391,8	540,0
wavenumber (1/cm)	3573,0	2916,0	1071,0	weak	841,0	1279,0
fundamental λ (nm)	2,80E-06	3,429E-06	9,337E-06	NA	1,189E-05	7,819E-06
n	**λ (nm)**	...				
1	2799	3429	9337	NA	11891	7819
2	1399	1715	4669	NA	5945	3909
3	933	1143	3112	NA	3964	2606
4	700	857	2334	NA	2973	1955
5	560	686	1867	NA	2378	1564
6	466	572	1556	NA	1982	1303
7	400	490	1334	NA	1699	1117
8	350	429	1167	NA	1486	977
9	311	381	1037	NA	1321	869
10	280	343	934	NA	1189	782
11	254	312	849	NA	1081	711
12	233	286	778	NA	991	652
13	215	264	718	NA	915	601
14	200	245	667	NA	849	558
15	187	229	622	NA	793	521
16	175	214	584	NA	743	489
17	165	202	549	NA	699	460
18	155	191	519	NA	661	434
19	147	180	491	NA	626	412
20	140	171	467	NA	595	391
21	133	163	445	NA	566	372
22	127	156	424	NA	540	355
23	122	149	406	NA	517	340
24	117	143	389	NA	495	326
25	112	137	373	NA	476	313
26	108	132	359	NA	457	301
27	104	127	346	NA	440	290
28	100	122	333	NA	425	279
29	97	118	322	NA	410	270
30	93	114	311	NA	396	261

Appendix A – continued

matching n_d	39,7	11,2	30,7	24,7	26,7
diss λ (nm)	197,1	540,0	197,1	540,0	540,0
wavenumber (1/cm)	1279,0	1652,0	1652,0	751,0	693,0
fundamental λ (nm)	7,819E-06	6,053E-06	6,053E-06	1,332E-05	1,443E-05

n	λ (nm)	...			
1	7819	6053	6053	13316	14430
2	3909	3027	3027	6658	7215
3	2606	2018	2018	4439	4810
4	1955	1513	1513	3329	3608
5	1564	1211	1211	2663	2886
6	1303	1009	1009	2219	2405
7	1117	865	865	1902	2061
8	977	757	757	1664	1804
9	869	673	673	1480	1603
10	782	605	605	1332	1443
11	711	550	550	1211	1312
12	652	504	504	1110	1203
13	601	466	466	1024	1110
14	558	432	432	951	1031
15	521	404	404	888	962
16	489	378	378	832	902
17	460	356	356	783	849
18	434	336	336	740	802
19	412	319	319	701	759
20	391	303	303	666	722
21	372	288	288	634	687
22	355	275	275	605	656
23	340	263	263	579	627
24	326	252	252	555	601
25	313	242	242	533	577
26	301	233	233	512	555
27	290	224	224	493	534
28	279	216	216	476	515
29	270	209	209	459	498
30	261	202	202	444	481

Appendix B – FT-IR spectrum of nitrocellulose (Giasson, 2005)

Note: Spectra shown on the next page.

NC sec Bergerac

Transmission / Wavenumber (cm-1)

File # 7 = NC SEC.TRANSMITTANCE
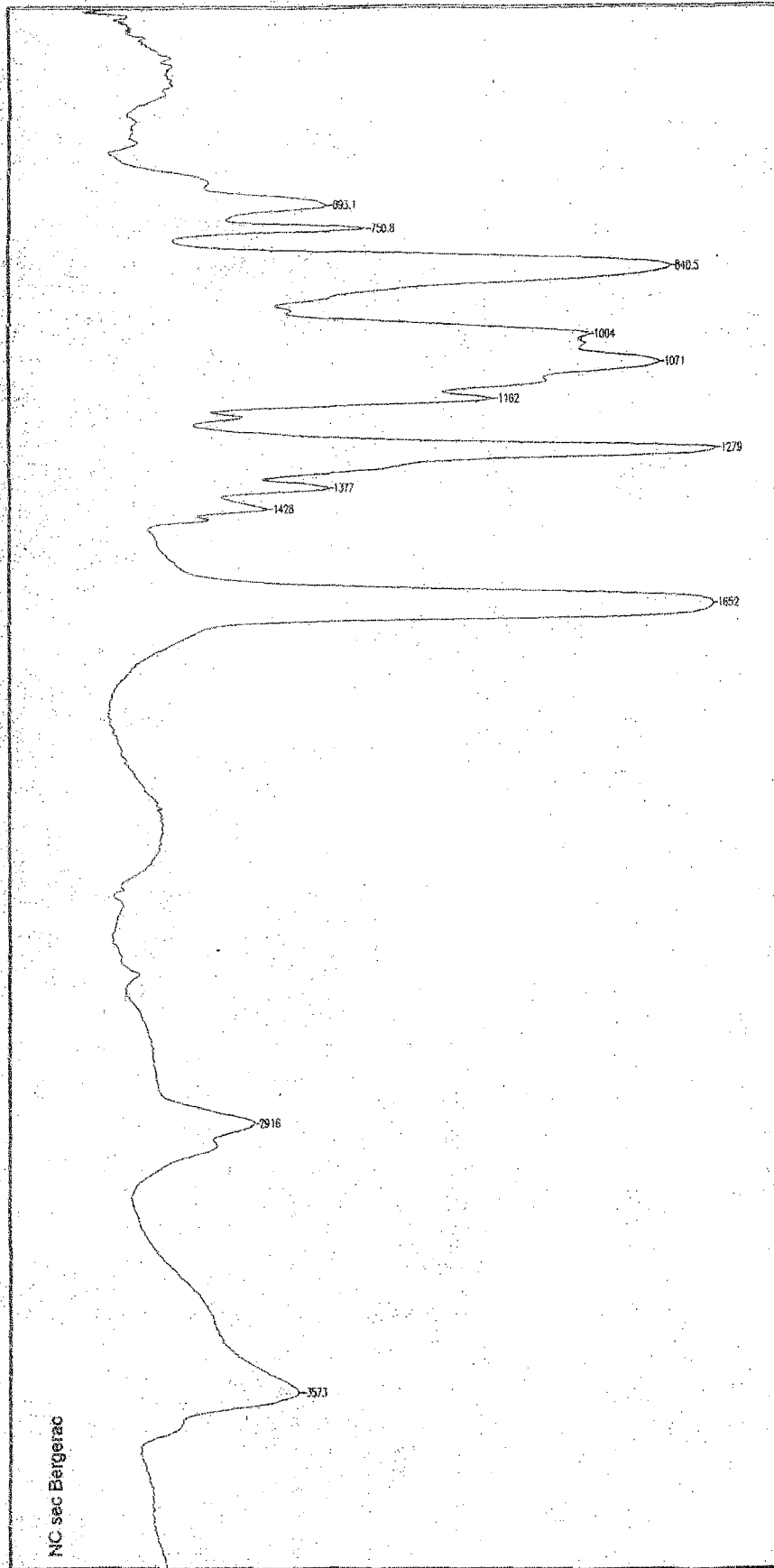
Bergerac

Paged Y-Zoom CURSOR

2005-12-21 10:32 Res=4